LABORATORY STUDY TO IDENTIFY THE IMPACT OF FRACTURE DESIGN PARAMETERS OVER THE FINAL FRACTURE CONDUCTIVITY USING THE DYNAMIC FRACTURE CONDUCTIVITY TEST PROCEDURE

A Thesis

by

ANDRES EDUARDO PIEVE LA ROSA

Submitted to the Office of Graduate Studies of
Texas A&M University
in partial fulfillment of the requirements for the degree of

MASTER OF SCIENCE

May 2011

Major Subject: Petroleum Engineering

Laboratory Study to Identify the Impact of Fracture Design Parameters over the Final Fracture Conductivity Using the Dynamic Fracture Conductivity Test Procedure

LABORATORY STUDY TO IDENTIFY THE IMPACT OF FRACTURE DESIGN PARAMETERS OVER THE FINAL FRACTURE CONDUCTIVITY USING THE DYNAMIC FRACTURE CONDUCTIVITY TEST PROCEDURE

A Thesis

by

ANDRES EDUARDO PIEVE LA ROSA

Submitted to the Office of Graduate Studies of
Texas A&M University
in partial fulfillment of the requirements for the degree of

MASTER OF SCIENCE

Approved by:

Co-Chairs of Committee,	Ding Zhu
	A. Daniel Hill
Committee Member,	Yuefeng Sun
Head of Department,	Stephen A. Holditch

May 2011

Major Subject: Petroleum Engineering

ABSTRACT

Laboratory Study to Identify the Impact of Fracture Design Parameters over the Final Fracture Conductivity Using the Dynamic Fracture Conductivity Test Procedure.

(May 2011)

Andres Eduardo Pieve La Rosa, B.S., Universidad Central de Venezuela

Co-Chairs of Advisory Committee: Dr. Ding Zhu
Dr. A. Daniel Hill

This investigation carried out the analysis of fracture conductivity in a tight reservoir using laboratory experiments, by applying the procedure known as the dynamic fracture conductivity test. Considering the large number of experiments necessary to evaluate the effect of each parameter and the possible interaction of their combinations, the schedules of experiments were planned using a fractional factorial design. This design is used during the initial stage of studies to identify and discharge those factors that have little or no effect. Finally, the most important factors can then be studied in more detail during subsequent experiments.

The objectives of this investigation were focused on identifying the effect of formation parameters such as closure stress, and temperature and fracture fluid parameters such as proppant loading over the final conductivity of a hydraulic fracture treatment. With the purpose of estimating the relation between fracture conductivity and the design parameters, two series of experiments were performed. The first set of experiments

estimated the effects of the aliases parameters. The isolated effect of each independent parameter was obtained after the culmination of the second set of experiments.

The preliminary test results indicated that the parameters with major negative effect over the final conductivity were closure stress and temperature. Some additional results show that proppant distribution had a considerable role over the final fracture conductivity when a low proppant concentration was used. Channels and void spaces in the proppant pack were detected on these cases improving the conductivity of the fracture, by creating paths of high permeability. It was observed that with experiments at temperatures around 250 $^{\circ}$F, the unbroken gel dried up creating permeable scales that resulted in a significant loss in conductivity.

The results of this investigation demonstrated that dynamic fracture conductivity test procedure is an excellent tool to more accurately represent the effects of design parameters over the fracture conductivity. These results are also the first step in the development of a statistical model that can be used to predict dynamic fracture conductivity.

DEDICATION

This thesis is dedicated to my mother, brother, and sister for all the love and support they have provided me throughout my life.

ACKNOWLEDGMENTS

I would like to express my sincere gratitude to my advisors, Dr. Ding Zhu and Dr. A. Daniel Hill, for giving me the opportunity to work under their supervision and for their encouragement, inspiration and support. Thank you both for your patience.

Thanks to Dr. Yuefeng Sun for serving as my committee member.

I would like to thank all the members of the Dynamic Hydraulic Conductivity Team: Juan Correa, Obadare Awoleke, Jose Romero and all the student workers who collaborated in this project.

I also want to extend my gratitude to John Maldonado for all his help, patience and support during this work.

Finally, I would like to thank the Harold Vance Department of Petroleum Engineering for giving me the opportunity to pursue my master's degree and to the Research Partnership to Secure Energy for America group for funding this research.

TABLE OF CONTENTS

Page

Page

LIST OF FIGURES

Page

Page

Page

LIST OF TABLES

Page

CHAPTER I

INTRODUCTION

1.1 Hydraulic Fracture in a Tight Gas Reservoir

In order to meet the growing energy demands, the exploration and production of hydrocarbon has increased across the world. However, due to the higher depletion rates of oil and gas reserves compared with the discovery of new reserves, the international energy sector is seriously thinking of developing unconventional energy sources such as, tight sands reservoirs, coalbed methane, and shale gas reservoirs (Zahid et al., 2007). Tight sand is a term commonly used to refer to low permeability reservoirs that produce mainly natural gas. In the 1970's the US government decided that the definition of a tight gas reservoir is a reservoir in which the expected values of permeability to gas flow is less than 0.01 md. However, a tight reservoir is a function of many physical factors, thus the best definition of tight gas reservoir is "a reservoir that cannot be produced at economic flow rates nor recover economic volumes of natural gas unless the well is stimulated with a large hydraulic fracture treatment." (Holditch, 2006).

_____

This thesis follows the style of *SPE Journal.*

Tight-gas reservoirs are found all over the world and occur in the most common types of reservoir rocks. Although the resource has been known for many decades, commercial development did not start until the 1970's when demand for natural gas increased, then prices rose, and drilling as well as completion technologies were improved. However, generalize that all types of tight reservoirs are the same is a very difficult thing to do, For instance this reservoirs can be found at shallow or deep depth, at low or high temperature, and can be a single layer or multiple layers. Due to all these differences a single and unique hydraulic fracture treatment cannot be designed and then be applied to all the different type of reservoirs (Holditch, 2006). Extensive work has been done over the previous decades to improve the success of fracturing treatments. The latest studies have been developed in order to recreate as similar the characteristics and procedures of a real fracture treatment to improve and avoid all the complications associated with the development of these reservoirs.

Hydraulic fracture treatments or "Frac Job", as it is commonly known in the oil industry, is the most common stimulation technique used to develop and produce tight sand reservoirs, but it is also widely used on high permeability reservoirs to bypass damage around the wellbore, and as a sand control technique. In this case the proppant pumped into the formation works as a filter reducing the pressure drawdown and preventing the sand to move into the wellbore. On this type of fracture treatment the fractures are designed to be short in length but large on width and height, different for what is expected during the hydraulic fracture treatment on low permeability reservoirs.

Hydraulic fracture treatments on low permeability reservoirs involve pumping large volumes of high viscosity fluid that are used to create an adequate width, large length and transporting the propping agent farther into the formation while minimizing the leak off into the formation. The injection of this viscous fluid causes the rock to break in a perpendicular direction to the least principal stress, creating a long, highly conductive path that increases the production rate until economical levels.

Since the first commercial hydraulic fracture treatment was performed in 1947 using gasoline-base napalm gel fracture fluid (Howard and Fast, 1970), the evolution of fracture treatments has provided the industry with numerous advances of sophisticated fluid systems, that increase and facilitate the transport of propping agent and reduce the leak-off into the formation. The most common type of treatment is performed using a guar-based crosslinked fluids, however, a large number of treatment have been successfully executed using slikwater or waterfrac. There are several differences between these two types of fluids, principally; the viscosity of the fluids that will have a major impact on the proppant transport. Also, the condition under these treatments executed are different, but regardless of all the differences, these two fluids have proven their success in creating highly conductive paths that will increase the production rate of gas (Palisch et al., 2007).

With the growth on energy demand the new era of engineering faces more complicated challenges. These challenges included the high costs to develop a tight gas reservoir, amount of technology, and engineer manpower. Therefore, new and modern studies

must be done. Studies should aim to reproduce more precisely the behavior of the fracture and more importantly represent and estimate with more accuracy the final fracture conductivity.

1.2 Literature Review

Since the first hydraulic fracture treatment was made, the goal of these treatments have been to create a long conductive path to increase the productivity of the well. In order to reach this goal two main tasks must be achieved. The first task is to create a long path. In order to create a long path it is necessary to inject a medium to moderate amount of high viscosity fluids or a large amount of low viscosity fluids. The second task is making this path conductive. To achieve this it is necessary that after the pumping process is finished the fracture be able to remain open and as clean as possible. After the first commercial use of the hydraulic fracture treatments in U.S., considerable effort has been devoted to increase its interpretation, performance, and its simulation under laboratory conditions (Howard and Fast, 1970).

Van der Vlis et al., (1975), performed a series of experiment to investigate how the placement of various proppant type and concentrations affects the conductivity, the fracture conductivity was calculated for mono-layer and multi-layers beds of proppant. Additionally during this research the transport of different proppant concentrations using low to high viscosity fluid were studied. The results concluded from this study state that high viscosity non-Newtonian fluids can transport proppant concentrations up to 8

lb/gal. However, the researchers found very difficult to reproduce the fracture conductivity measurements.

McDaniel (1986) conducted a series of experiments with the objective of investigating the combined effect of temperature and closure stress for long periods of time. These experiments were performed using the conductivity test cell and apparatus described in 3rd draft of the "Recommended Practices for Evaluating Proppant Conductivity" (API RP 61). This research concluded that laboratory measurements of conductivity at ambient temperature and for short periods of time resulted in optimistic values. On the contrary for an extended period of time the effect of closure stress and temperature resulted in a correction factor around 0.6 and 0.3 respectively over the conductivity.

The American Petroleum Institute developed and published recommended practice guidelines known as API RP 61 (1989); this recommended practice describes how to obtain the conductivity of proppant using a conductivity cell. The conditions for the test include the following: ambient temperature, a proppant concentration around 2 lb/ft^2, and the closure stress should be maintained for 15 hours. After several investigations the researchers realized that the procedure presented in this manual resulted in optimistic values of conductivity and a longer term test will need to develop to better simulate reservoir conditions (Flowers et al., 2003; Palisch et al., 2007). These investigations were sponsored by StimLab and some of the major changes done to the initial procedures include, replacing the original steel piston for Ohio sandstone, increasing the temperature to $150^{\circ}F$ or $250^{\circ}F$, and maintaining the closure stress for as long as 50

hours. These changes affected substantially the results of the proppant conductivity test reducing the final conductivity by as much as 85% (Palisch et al., 2007). Finally in 2007, the standard for long-term conductivity testing came to be known as the ISO 13503-5 (Kaufman et al., 2007).

Milton-Taylor (1993) carried out a laboratory study to evaluate the factors affecting the stability of proppant and possibility of proppant backflow in the fracture. A channel on top of the proppant pack was used to investigate the proppant backflow. The results of this investigation showed that embedment of proppant into the rock play a key role in stability of proppant. This study however, was performed without the use of any fracture fluid inside of the cell.

Dewprashad et al. (1999) performed a laboratory study as well as field testing to demonstrate that it was possible to increase the conductivity of the fracture by modifying the surface of the proppant pack. During this study different polymeric “tackifiers” were used to prevent the movement of proppant and avoid the backflow of proppant into the wellbore. The experiments were carried out using a modified API conductivity cell and a syringe pump to maintain a constant flow during the experiment. Their experiments were successful, however, the inside of the conductivity cell was loaded manually allowing the proppant to settle in a homogeneous form and this circumstance does not represent the reality in a fracture treatment.

New experiments have been carried out with the goal of better representing the behavior of the proppant under different reservoir conditions. This is the case of the study performed by Schubarth and Milton (2004). In this investigation the behavior of proppant at different stresses conditions were performed. During the experiments different types of proppant were tested to understand the relationship between the increment of the closure stress and conductivity of the proppant pack. The tests were performed using an API crushing cell, where the proppant was placed manually and in equal concentrations of 2 lbs/ft^2. The results reached during this study revealed that ceramic proppant and sand do not crush in the same way. A relationship between the median particle diameters and the permeability of the proppant packs were obtained. Their experiments did not consider the effect of temperature or embedment of particles on the rock. They simply left the cell at the desired closure stress for a determined time without flowing any fluids a condition that can alter the distribution or removal of any crushed material.

Palisch et al. (2007) studied and analyzed how the proppant crush test can be misused. During their work, the researchers analyzed and compared the results obtained when a standard crush test and a standard conductivity test are performed to estimate the final conductivity of the proppant pack. The experiments were carried out using three popular 20/40 proppants. The results showed that significantly greater proppant damage was experienced during the standard conductivity test where the proppant was compressed between two pieces of rock instead of two metal pistons. This study concluded in the

necessity to conduct new experiments that represent more closely downhole conditions where, the non-Darcy flow, multiphase flow, gel damage, higher temperature, and higher closure pressure are examined to represent and obtain more realistic results.

Nowadays, the improvements on stimulations treatments have made the development of the unconventional reservoirs possible. These reservoirs were once considered uneconomical to produce due to the lack of technology. These developments have contributed with the continued increase in energy demand (Zahid et al., 2007). As the energy sector faces new challenges to make these stimulation treatments more efficient and finding out the way to reproduce them with more exactitude in the laboratories becomes important. Because of this, new experimental work as the one performed by Marpaung (2007) and Pongthunya (2007) have been carried out. During these experimental studies a new apparatus to perform dynamic hydraulic fracture experiments was designed and assembled. This experiment is different from the conventional fracture conductivity test, where the proppant is place by hand. The new apparatus was assembled and tested and allowed researchers to perform the placement of the proppant dynamically at the same time as the slurry is pumped into the fracture conductivity cell. This process simulates more closely the field conditions of the fracture treatment. This new equipment was built based on a modified API conductivity cell and designed to accommodate two cores of 3 in. of height and a cross area of 12.5 in^2. Also the new cell has two side pistons with leak-off ports to measure the fluids leak-off during the clean up process.

Marpaung (2007) studied the effect of gel residue on hydraulic fracture conductivity performing a series of experiments using the new dynamic hydraulic fracture apparatus. During his experiments Marpaung examined different scenarios using hydraulic fracture fluids with polymer concentrations from 30 lbm/Mgal to 50 lbm/Mgal at a constant temperature and closure stress of 150°F and 2000psi respectively. This laboratory study concluded that increasing polymer concentration decreases fracture conductivity for a constant gas flow rate, and a lower gas flow rate reduce the cleanup of the fracture resulting on a lower final fracture conductivity. Experiments without breaker were conducted as well they showed the damaging effect of viscous hydraulic fracturing fluids without breaker on the conductivity of the proppant packs. It was also concluded that static conductivity tests resulted in higher retained fracture conductivity when compared to dynamic conductivity testing.

There has been significant progress and efforts made to realistically evaluate and quantify the behavior of proppant-pack conductivity due to gel damage, although very little has been disclosed to study the effect of reservoir conditions necessary to increase fracture conductivity. This research, therefore conducted a series of experiments to identify the effect of temperature in a range of 150 $^{\circ}$F to 250 $^{\circ}$F, proppant loading in a range of 0.5lbm/Mgal to 2lbm/Mgal and closure stress in a range of 2000psi to 6000psi, over the final conductivity of the fracture. Therefore it is possible to identify which factor or set of factors have had a major impact over the fracture conductivity.

Additionally, these results are being used as a first step in the development of a statistical model that can then be used to predict future dynamic fracture conductivities.

1.3 Research Objectives

1. Conduct a series of experiments to determine the effect of temperature, closure stress, and proppant loading over the final conductivity that will be measured using low permeability rock and wet gas.
2. Analyze the effect of temperature, closure stress, and proppant loading using the factorial design procedure.
3. Identify the performance of lightweight ceramic proppant under simulated reservoir conditions using the dynamic conductivity test procedure.
4. Evaluate the effect of closure stress and temperature over the embedment and crushing of lightweight 30/50 ceramic proppant.

By completing the above objectives, this research will be able to estimate more accurately the conductivity of a hydraulic fracture treatment in tight gas formations based on experimental work.

Additionally, this study presents a better understanding on how design parameters affect fracture conductivity in tight gas formations, which will help in future designs of fracturing treatments and future predictions of well performance and productivity.

CHAPTER II

EXPERIMENTAL SET UP, PROCEDURES, AND CONDITIONS

2.1 Experimental Set Up

The state of the art dynamic fracture conductivity apparatus used in this research was previously designed and assembled by Marpaung and Pongthunya (2007). This experimental set up is divided into three parts; the hydraulic conductivity cell, the pumping setup, and the fracture conductivity measurement setup. The laboratory and parts used in this study provides proper scaling to represent the actual field conditions on an experimental level.

The hydraulic conductivity cell used during this project is a modified API RP-61 (1989) conductive cell. This modified cell has several similarities with the original recommended cell illustrated on Fig. 2.1. Both cells allows linear flow through the proppant pack, both have three ports for pressure measurement, and two side pistons used to maintain the cores in place and to pass the closure stress onto the proppant pack. However, several differences have been included in the new conductivity cell. The new cell structure is able to accommodate core samples of 7 in. long, 1.7 in. wide, and 3 in. height, with a 12.5 in^2 bed area, and two 12 in. height side pistons with leak-off ports to allow the flow of liquid through the cores during the test if it is needed. Fig. 2.2 illustrates the modified conductivity cell used during the realization of this project.

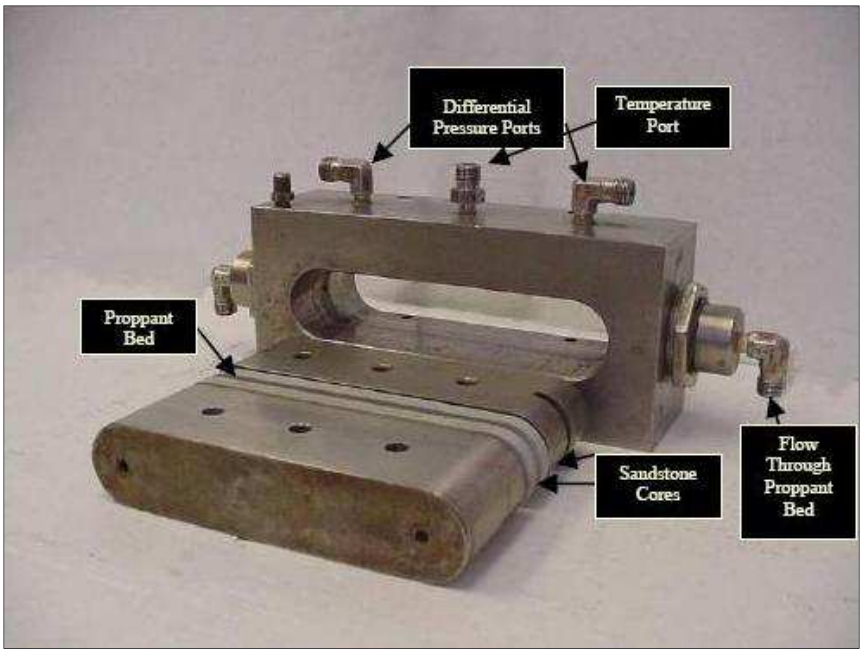

Fig. 2.1 API RP-61 hydraulic conductive cell (Palisch et al., 2007)

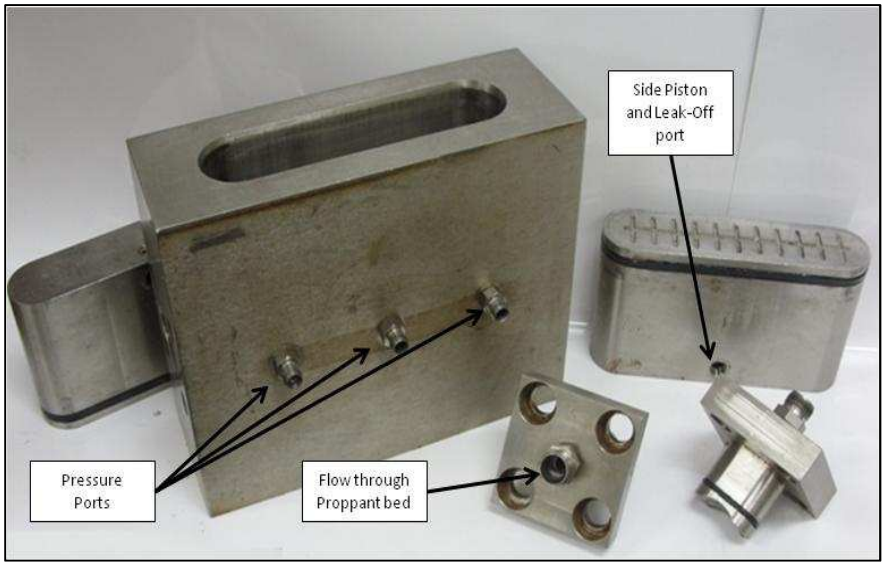

Fig. 2.2 Modified conductivity cell for dynamic conductivity test

The schematic of the pumping setup is shown in Fig. 2.3**.** Looking at this figure it is possible to observe three main sections. The first section is the mixer section; this section consists of two tanks, the mixer tank and the pumping tank. The mixer tank is used to prepare the base gel. Once the base gel has been hydrated after a period of time no less than 30 minutes it is pumped to the pumping tank and then into the conductivity cell. This initial base gel is pumped into the conductivity cell to recreate the injection of pad as it is injected into the reservoir. Meanwhile, on a side, the slurry mixture is prepared in a 5 gallons bucket using a paddle mixer to guarantee the creation of a vortex and the identification of the exact point when the gel has reached the crosslinked point.

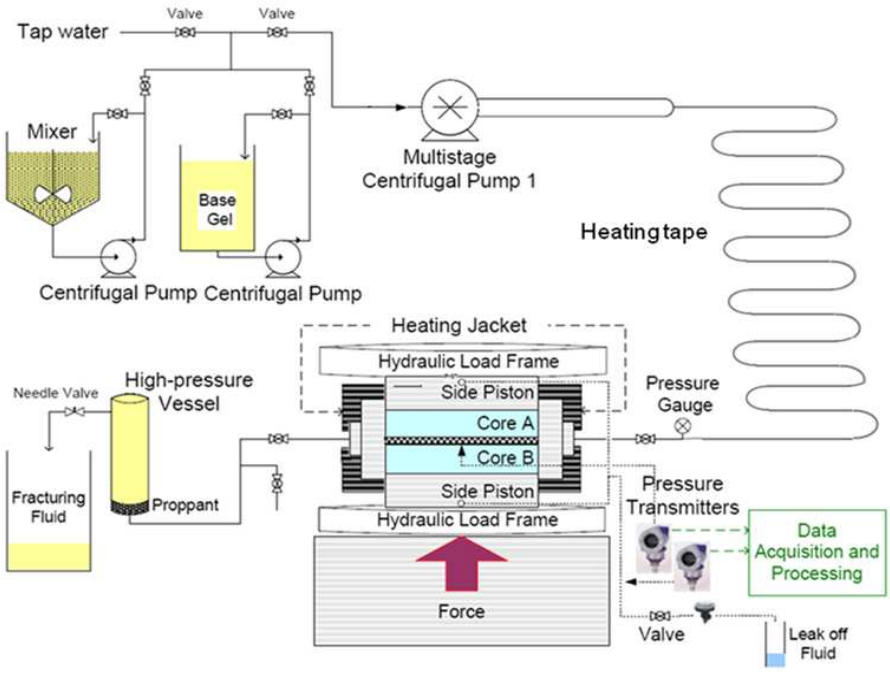

Fig. 2.3 Pumping schematic of dynamic fracture conductivity test (After Marpaung 2007)

The second section is the pumping and heating section. This section consists of three centrifugal pumps to mimic field treatment conditions. Two of these pumps are use to displace the base gel and slurry mixture from the tanks into the multistage centrifugal pump. This pump is used to move both fluids around the entire system and keep the pressure inside the conductivity cell at a constant 700 psi. To extend the lifetime of these pumps all of them are flushed with at least 5 gallons of base gel and water to remove as much of the remaining proppant as possible. Since temperature is considered one of the main factors during this study, changes were performed to increase the efficiency of the heating section. In the previous setup cylindrical heaters were used to pre-heat the fluids on its way into the conductivity cell. These cylindrical heaters were inefficient since its radius was bigger than the tubing used on the setup. In the present setup a heating tape is wrapped around the tubing to heat up the fluids to a temperature of 150 $^{\circ}$F before it reaches the conductivity cell. Additionally, a heating jacket is used around the conductivity cell to simulate the temperature at reservoir conditions and to help the slurry to fully break inside the cell.

The final section is the data acquisition and loading frame section. This section consists of two rugged and reliable Validyne DP15 sensors. These sensors provide superior accuracy for measuring low-pressure liquids and gasses while it withstands the abuses of

laboratory testing. This type of sensor allows the use of different diaphragms that ranges from 0.08 psi to 3200 psi depending on the requirements of the experiment. Fig. 2.4 illustrates how the sensors are connected within the conductivity cell. The use of filters and valves in front of the sensors are important to prevent the flow of proppant that can cause a malfunction of these sensors. The sensors measure the differential pressure and absolute pressure during the entire time of the experiment. The sensors are connected to the loading frame's computer. A robust loading frame system is used to apply the desired closure stress to the proppant pack and to place the upper core into its final position. Fig. 2.5 shows an image of the software used to control the loading frame as well as monitor the pressure sensors readings. This software allows the researchers to maintain a constant supervision on the closure pressure, the changes of absolute pressure and differential pressure, and the movement of the piston that can be directly correlated to the closure of fracture width.

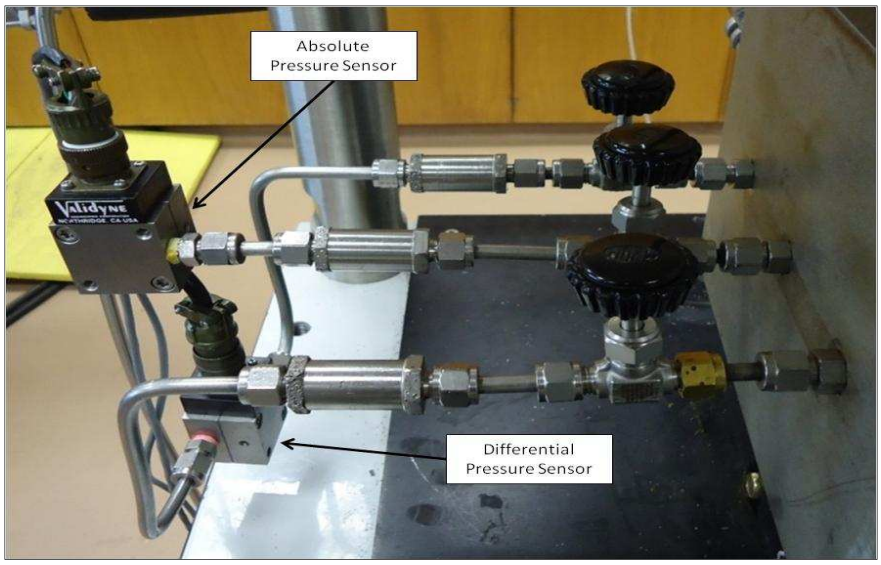

Fig. 2.4 Pressure sensors used in the conductivity cell

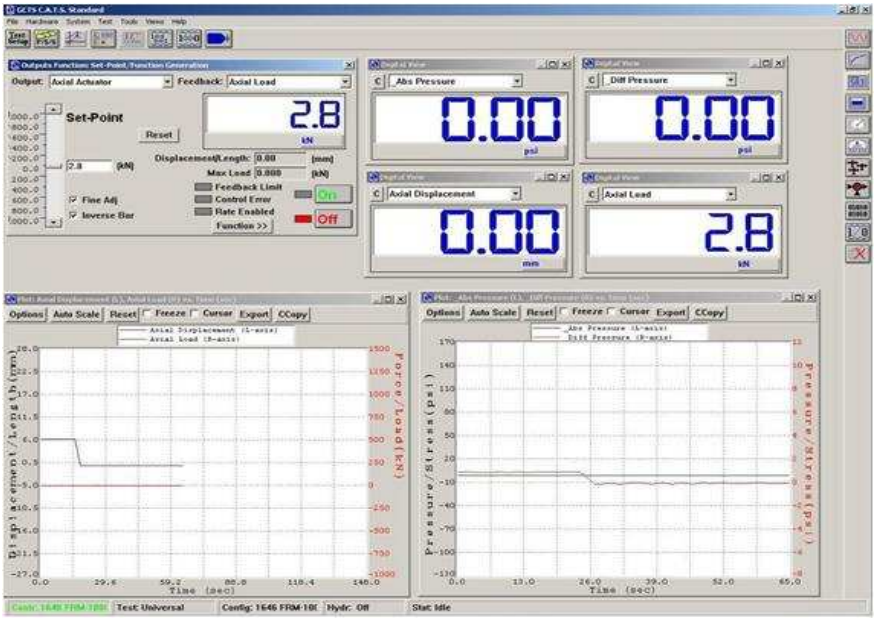

Fig. 2.5 Reference view of GCTS C.A.T.S. control software

The entire equipment used during this research is summarized below:

- A mixing tank - to prepare the base gel
- A pumping tank
- 5 gallon bucket and paddle mixer - to prepare slurry mixture (gel and proppant)
- High pressure centrifugal pumps
- Heating tape and heating jacket - to increase the temperature to reservoir conditions
- Modified API RP-61 fracture conductivity cell
- High-pressure accumulator
- GCTS loading frame to apply a load stress
- Data acquisition system connected directly to the GCTS loading frame to collect parameters such as: absolute pressure, differential pressure, closure stress and displacement.
- Nitrogen cylinder and water accumulator used to wet the gas before it flows into the cell
- A loading frame to apply a load stress

2.2 Experimental Procedure

Accurate fracture conductivity measurements are the key to this research. After careful investigation and study the experimental procedure was developed in six consecutive steps. Each step involved in this process is mentioned on Fig. 2.6. The description of each step is explained below.

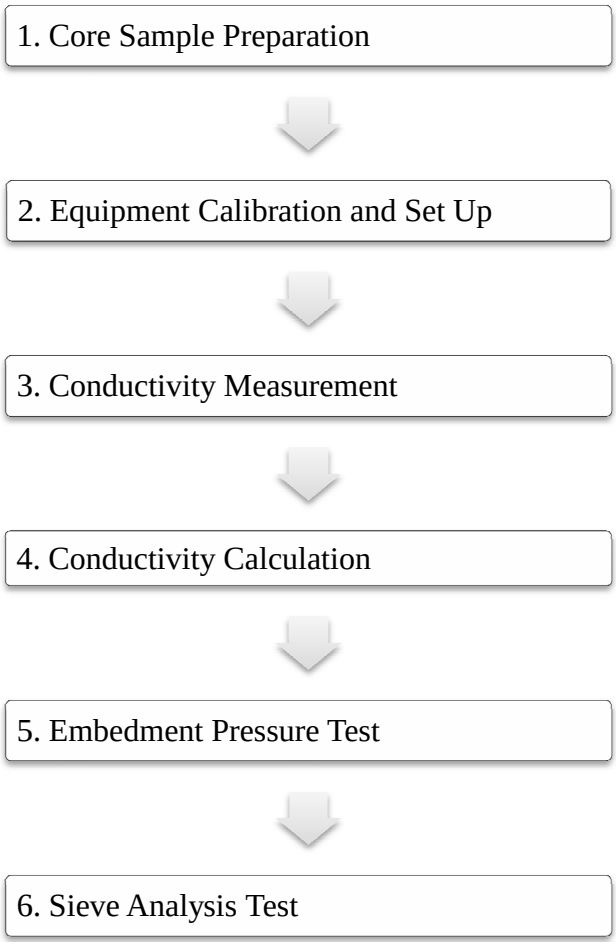

Fig. 2.6 Experimental procedure for dynamic fracture conductivity testing

2.2.1 Core Sample Preparation

The core samples used during this research are made from low permeability Ohio Scioto sandstone that have been custom cut to fit into the modified conductivity cell. The dimensions of these cores are 7 in. long, 1.65 in. wide, and 3 in. in height. The preparation consists of covering the sides of the cores with a silicon base mixture to create a seal and a perfect fit between the rock and the walls of the conductivity cell. Fig. 2.7 shows the cores before and after the silicon mixture is applied.

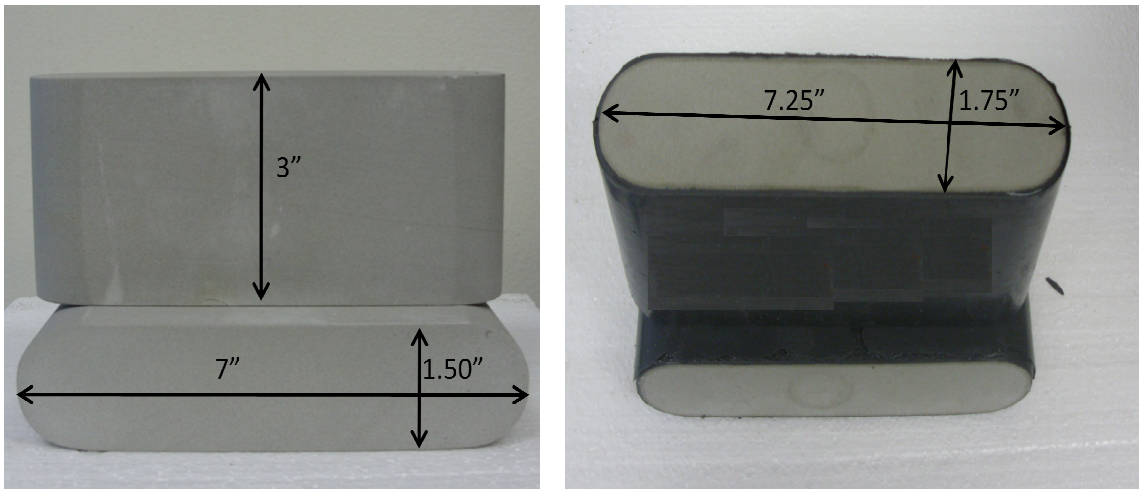

Fig. 2.7 Core samples before and after covered with the silicon mixture

The detailed core sample preparation procedure is as follows:

1. Put tape on top and bottom surface, and cut edges with razor cutter.
2. Apply two layers of the silicone primer (SS415501P). Allow 15 minutes waiting time in between layers.
3. Clean metal surface and bottom plastic part of mold with cloth and stoner spray. Fig. 2.8 shows the mold structure used. It is made of stainless steel, with a plastic bottom.
4. Assemble mold and screw the 4 bottom and the 3 side screws.
5. Place rock in mold and adjust to center position.
6. Mix 1 part of silicone potting compound with 1 part of silicon curing agent, and weigh before mixing the second component to make sure the mixture is 50/50 of each component, either by volume or by weight percent.
7. Using disposable syringes pour mixture in mold carefully until filled to the top without spilling over the sides.
8. After filling the mold to the top, clean the outside of the mold to prevent from dripping any extra silicon mixture.
9. Place sample in an oven and set the temperature to 100°C, wait approximately 1 hour.
10. Disassemble the cell and extract core sample.
11. Cut the extra silicon left on the edges of the core with a razor cutter.
12. Label and store the rock sample.

Fig. 2.8 Stainless steel mold used to prepare the cores

2.2.2 Equipment Calibration and Set Up

The equipment calibration consists of the initial calibration of the fracture width and pressure sensors. These calibrations have to be done every time before each one of the experiments to guarantee reliable results. A known initial fracture width is important for the calculation of the final permeability of the fracture. The measurement of the initial width starts with the assembling of the bottom core into the conductivity cell. Insert the bottom core sample through the bottom opening of the conductivity cell using a hydraulic press. Make sure the lower fracture face lines up with the bottom of the pressure ports in the cell. This will guarantee that the proppant pack is in the center of the cell and both cores and side pistons can fit properly with a good seal.

For the upper side of the conductivity cell a similar procedure is applied. The upper core is initially placed by hand and later with the help of a hydraulic press placed inside the cell. The initial width is then measured using a metal bar of 0.25 inches (6.35 mm) of width. The final placement of the cores is made with the loading frame. The detailed procedure for setting up the final width of conductivity cell prior to pumping is as follows:

1. Using the CATS software, activate the output function tool.
2. Select the proper feedback *Axial Displacement* for this setup**.**
3. Using the arrows for a small change or typing the number for a larger displacement start moving the loading frame piston until the conductivity cell fits under it.
4. Once the conductivity cell is centered under the loading frame's piston, bring the piston down slowly until it makes contact with the upper conductivity cell's piston.
5. Start displacing the loading frame's piston until the upper core touches the metal bar.
6. Applying slight pressure removes the bar and then uses the triangular ruler to make sure that both sides have the same opening of 0.25 inch (6.35 mm). Fig. 2.9 shows what the triangular ruler looks like.
7. Fig. 2.10 shows how the cell should looks after it is assembled.

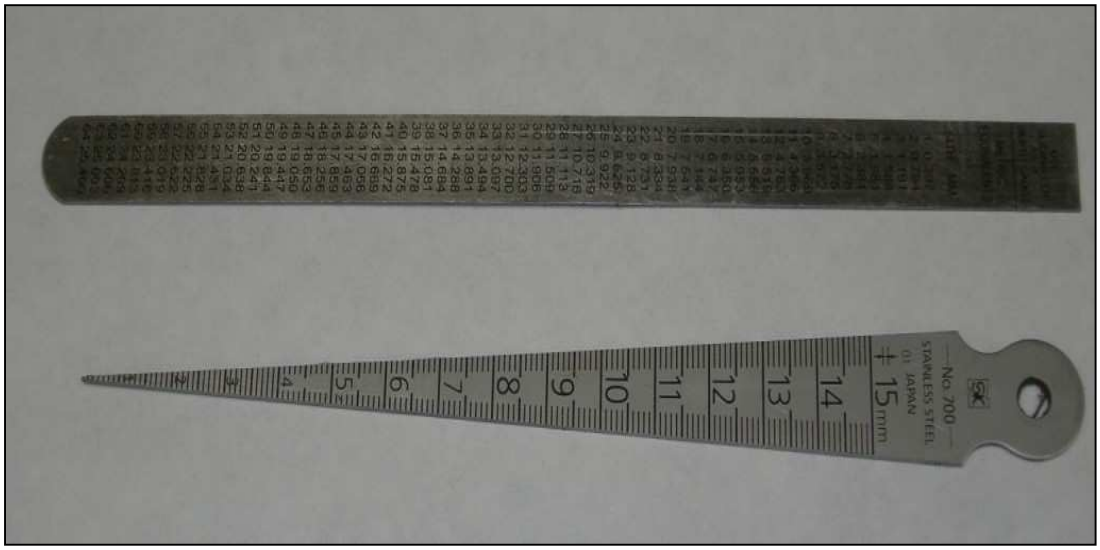

Fig. 2.9 Triangular ruler used to measure the distance between the cores

Fig. 2.10 Final assembly of the modified conductivity cell

For an accurate conductivity measurement the proper pressure must be measured inside the conductivity cell. Absolute pressure and the differential pressure inside the conductivity cell are going to be digitalized and recorded using the data acquisition system. For this study easy to replace pressure sensing diaphragm that are contained in one compact unit are used. Using GCTS's software it is possible to monitor and record the pressure behavior. However, in order to guarantee the accuracy of these sensors is recommended to test them and calibrate them before every experiment as necessary.

A detailed guideline for the calibration process is presented below:

1. Connect the pressure sensor's high pressure port to the pressure gun. Test the pressure sensor to read several pressures. Compare the pressure on the gauge attached to the pressure gun with the pressure reported in the CATS sensor reading windows. If the sensor is calibrated continue to connect the sensor to the conductivity cell. If the sensor is not calibrated follow the following procedure.
2. On the upper menu of CATS' software locate and click on *System, Input, and Analog.*
3. From the *Analog Inputs* window select which of the pressure sensors you want to calibrate (Absolute or Differential pressure).

4. Once it is selected, click *Edit*. Editing Analog Inputs windows will pop-up. See Fig. 2.11.
5. Make sure that the maximum and minimum values of the sensors are correct (In case you are using different diaphragms).
6. Click on *Calibrate* button and select *Two points Calibration.* See Fig. 2.12.
7. Make sure that no pressure is been applied to the sensor. Open the bleeding port of the high pressure side. Type the number zero (0) on the first box and click *Next.*
8. Add the desired pressure and type the pressure read on the gauge attached to the pressure gun in the second box and click *Next.*
9. Steps 7 and 8 must be repeated one more time. When completed that click *Close* and *Ok*. Make sure that the pressure read on the sensor reading windows is the same as the reading on the gauge attached to the pressure gun.
10. Unplug the sensor and continue with the testing and calibration of the second pressure sensor

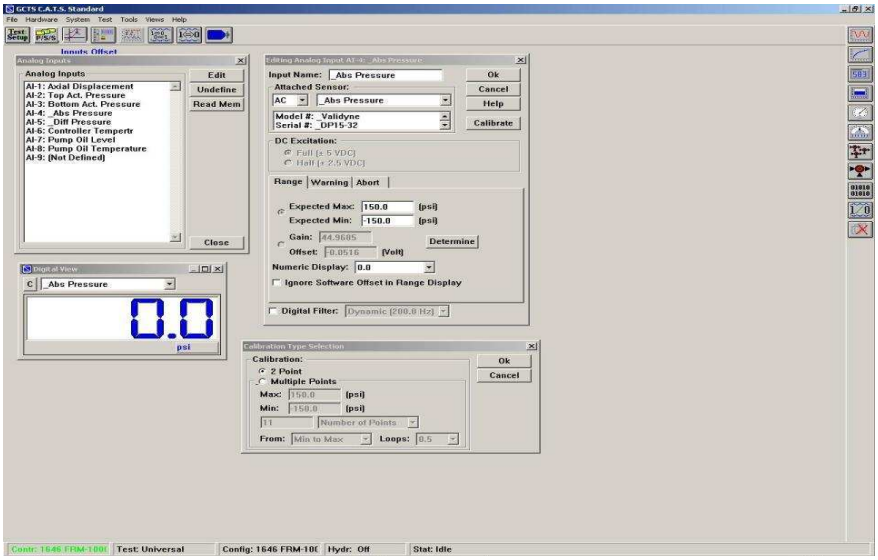

Fig. 2.11 Reference view of the calibration windows on GCTS C.A.T.S software

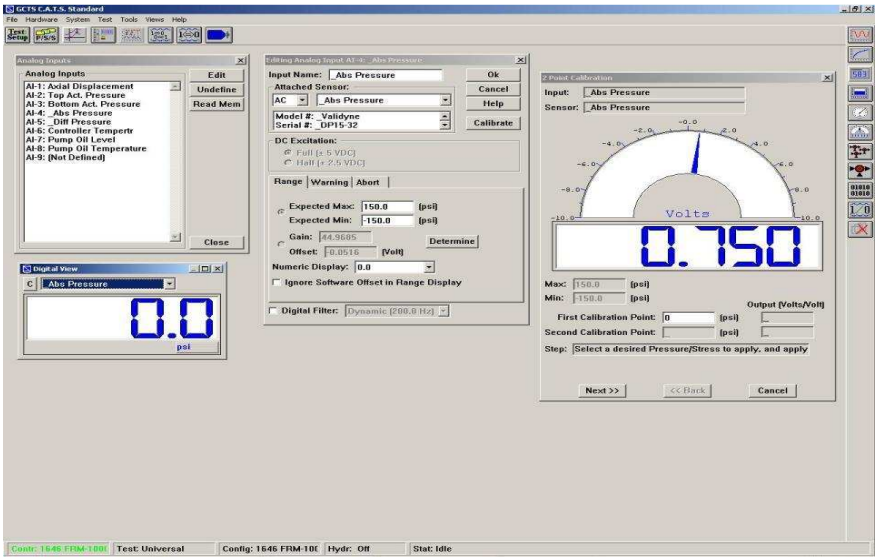

Fig. 2.12 Reference view of the two point calibration windows on GCTS C.A.T.S software

2.2.3 Conductivity Measurement

During this study the fracture conductivity was measured using a similar procedure to the one used by Marpaung (2007). This procedure is a continuous process which begins by pumping slurry. Below is the procedure for measuring the fracture conductivity.

1. Calibrate the mass flow controller to zero by adjusting flow controller to the closed position and wait until the reading is zero.
2. Use C.A.T.S software to record pressure from the pressure transducer. Write down any initial value in the transducer, this value will be important to calibrate the conductivity table.
3. Open the nitrogen regulator and mass flow controller to flow gas into the conductivity cell.
4. Check all lines for leakage. Close the nitrogen regulator if leakage is found and repair the leak.
5. Adjust nitrogen regulator, the back pressure valve, and mass flow controller until the cell pressure reading reaches 50 psi and the gas flow rate reaches ± 2 slm.

6. Wait until flow rates and pressure readings stabilize and record the gas flow rate, cell pressure, and differential pressure.
7. Vary the gas flow rate from 2 to 10 slm to get five data sets at cell pressure ± 50 psi. To increase gas flow rate, open the nitrogen regulator.
8. After reading 5 points, reduce the flow rate until reaches the desire cleanup flow rate.
9. Continue the flow of nitrogen at a low predetermined rate for a predetermined time.
10. Repeat Step 6 to 9 every two hours to get data points for the fracture conductivity calculation.
11. Turn off the nitrogen flow and disconnect all lines to the conductivity cell.
12. Remove the rock sample from the cell with the hydraulic jack.
13. Collect the proppant from the faces of the core, weight and record the mass.
14. Calculate the fracture conductivity by using Forcheimer's equation (Equation 2.1).

2.2.4 Conductivity Calculation

The fracture conductivity is going to be calculated using the Forcheimer's equation. This equation can be rearranged to obtain the equation of a straight line (Equation 2.1). Values of flow rate, absolute pressure and differential pressure are measured as explained on Section 2.2.3. With the combination of these factors and the parameters reported on Table 2.1 it is possible to calculate the X and Y components at different periods of time. The fracture conductivity can be now calculated by the inverse of the intercept of the straight line with the y-axis. Table 2.2 and Fig. 2.13 demonstrated an example of the use of the Forcheimer's chart.

$$\frac{\left(p_1^2\text{-}p_2^2\right)Mh}{2ZRTL\mu\rho q}=\frac{1}{wk_f}+\frac{\beta\rho q}{w^2\mu h} \qquad \text{Eq. 2.1}$$

Table 2.1 Experimental constants used for the Forcheimer's equation

M	Molecular mass of nitrogen, Kg/Kg mol	0.028
H	Height of fracture face, in	1.61
Z	Compressibility factor	1.00
R	Universal constant, J/mol K	8.32
L	Length of fracture over which pressure drop is measured, in	5.25
μ	Viscosity of nitrogen at standard conditions, Pa.s	1.747E-05
ρ	Density of nitrogen at standard conditions, Kg/m^3	1.16085

Table 2.2 Parameters used to calculate the conductivity using Forcheimer's equation

Flow Rate (slm)	Absolute pressure P_{Cell} (psi)	Differential pressure ΔP (psi)	y-axis, $(P_1^2-P_2^2)Mh/(2ZRTL\rho\mu q)$ $(1/m^3)$	x-axis, $rq/h\mu$, no unit
2.1	49.5	0.4	6.54318E+12	51.958
4.2	53.9	0.86	7.516E+12	103.915
6.3	59.2	1.35	8.47327E+12	155.873
8.1	63.62	1.77	9.15745E+12	200.408
9.7	67.5	2.08	9.43141E+12	239.995

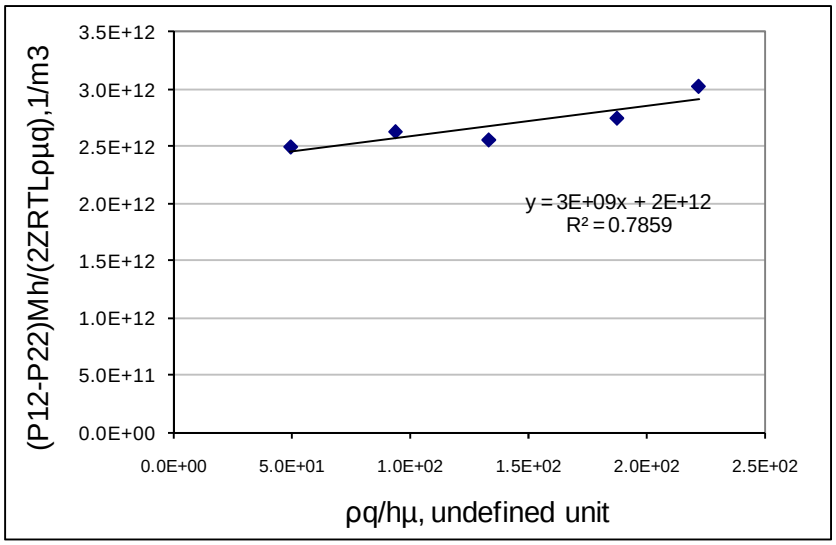

Fig. 2.13 Forcheimer's chart used to calculate fracture conductivity

2.2.5 Embedment Strength Test

The embedment pressure was calculated following the procedure described by (Howard and Fast, 1970). In this method the embedment of the rock is calculated using a steel ball with a determined diameter. With the use of a hydraulic press and a displacement measurement instrument, the steel ball will be embedded into the rock to a depth of half of the radius of the ball. The load needed to embed the ball is then recorded. This procedure must be repeated at least three times with a distance of 1/2 inch between each one of them. Equation 2.2 shows the embedment pressure equation from (Howard and Fast, 1970).

$$S_{re} = \frac{4W_p}{\pi d_i^2} \qquad \text{Eq. 2.2}$$

W_p is the load applied and d_i is the diameter of the steal ball.

Fig. 2.14 shows the rock embedment strength measurement apparatus. The apparatus has two different gauges, the top gauge measures pressure reading and the bottom gauge measures the indentation distance. Fig. 2.15 shows the points where the test was carried out.

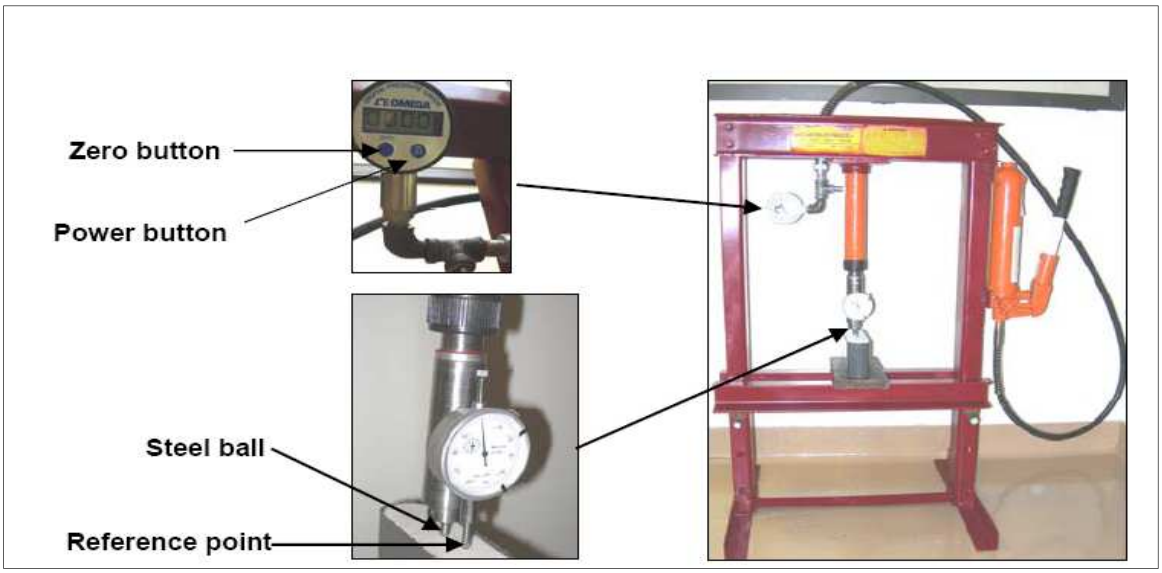

Fig. 2.14 Rock embedment pressure apparatus operated with a hydraulic oil piston (After Melendez-Castillo 2007)

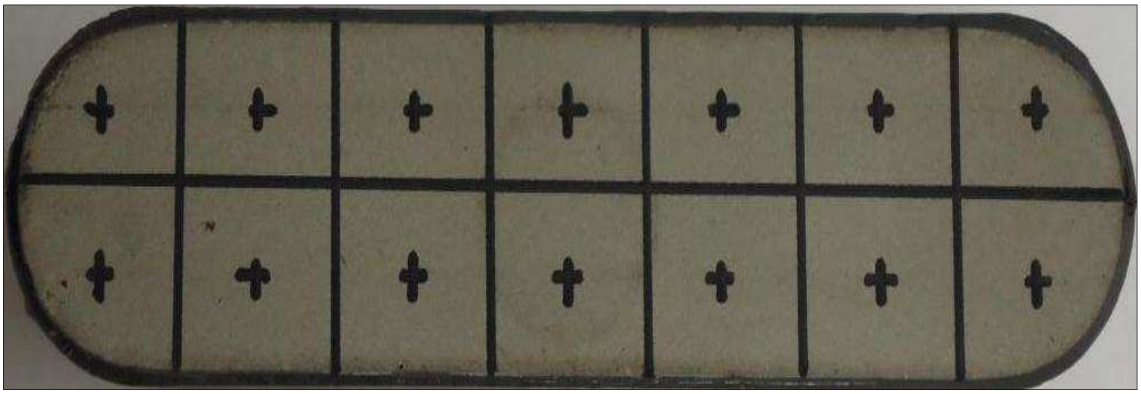

Fig. 2.15 Core surface with the points position for the embedment pressure test

We measured the rock embedment strength at 14 different points on the surface of the core. The detailed hardness measurement procedure is as follows:

1. Use a guide to mark the points of measurements on the surface of the rock. Place the rock sample in the rock embedment strength base and bring down the steel ball until it is touching the rock surface without applying any pressure.
2. Place the needles from the indentation distance's gauge device into the zero position. Press the zero button in the pressure gauge if the gauge does not show a zero value in its screen.
3. Indent the steel ball to a fixed distance of 0.016 inches, read the pressure required for the indentation, and record the reading on the control sheet.
4. Repeat Steps 1 to 3 for all the measurement points.

2. 2. 6 Sieve Analysis

Most proppant choices are currently based on which one has the highest baseline conductivity, lowest cost and availability (Terracina et al., 2010). To identify the effect that crushed proppant over the final conductivity of the proppant pack, a sieve analysis was performed. After the sieve analyses we were able to obtain a more accurate representation of the proppant performance under downhole conditions of temperature, pressure, and rock properties.

The detailed procedure for sieve analysis is as follows:

1. Inspect all the equipment to be used and clean any equipment that has proppant samples or other debris left in it.
2. Measure the mass of the proppant sample to be used in the experiment.

3. Select the first five large mesh sieves (20-30-40-50-70). Individually weigh each of the sieves.
4. Stack the selected sieves according to mesh size. The sieve number can be located on the side of the sieve (for example 20, 30, and 40). The largest of the sieve numbers should be on the bottom. Place the fine collector on the bottom of assembly
5. Apply the spring-loaded top of the assembly and secure it to the arms of the bottom assembly. The assembly should be similar to Fig. 2.16
6. Place the entire assembly in the sonic sifter. The spring-loaded top needs to be pushed down to fit inside the sifter.
7. Slide the assembly into the sifter and allow the switch on the left side to flip back.
8. Close the door of the sifter.
9. Turn on the power toggle switch.
10. Turn the main time knob to 15 minutes and press the start button.
11. Allow the sifter to run for the selected 15 minutes; it will stop when the timer is finished.
12. Gently remove the sifter apparatus from the machine. Weigh each individual sieve and record the data. The difference between the empty weight and the weight after sifting is the volume of proppant trapped in the sieve.

Fig. 2.16 Final assemble of the sieve analysis equipment

2.4 Factorial Experimental Design

The realization of an experimental work requires a large number of experiments. The numbers of experiments are proportional to the number of factors that the researcher is interested to investigate. One of the most common procedures applied during experimental work is the evaluation of one factor at the time. This process has proved to be consistent but time consuming, especially if a large number of experimental variables are involved. The efficiency of this procedure however, comes at a great cost. Experiments designed using the one factor at a time cannot estimate the interaction between factors.

In general, factorial (2^k) experiments are used to overcome the above mentioned limitations. However, the number of experiments required to completely characterize the main and interaction effects in a factorial experiment grows in an exponential fashion as the number of factors increase. Therefore, when a large number of factors are to be investigated, the researcher could consider and examine the use of fractional factorial design. This type of design is among the most widely used type of design that are used in the industry given its efficiency and utility. A major use of factorial designs is the use of the screening process at experiments (Myers and Montgomery, 2002). These are experiments in which many factors are investigated with the purpose of identifying those factors (if any) that have a large effect on the response variable. This type of experiment is carried out during the initial stage of the study to identify and discharge those factors that have little or no effect on the response. Finally, the most important factors can be studied in more detail during subsequent experiments.

The successful use of the factorial designs is based on three principles that have been validated in an empirical way. This meaning that their validity was confirmed based on experience rather than being proved theoretically. The three principles are as follows:

- *Hierarchical ordering principle*: This principle states that lower order effects are more likely to be important than higher order effects and effects of the same order are equally likely to be important.
- *Effect sparsity principle:* This principle states that the number of relatively important effects in a factorial experiment is small.
- *Effect heredity principle:* This principle states that the order for an interaction to be significant, at least one of its parent factors should be significant.

A factorial design involves the study of factors at different levels. During this project all the factors were analyzed at two levels, therefore the using the fractional factorial design. A fractional factorial design can reduce the number of runs required for an experiment by providing as much useful information at even greater economy. In general, a 2^k design may be run in a $1/2^p$ fraction called 2^{k-p} fractional factorial design. Thus, a 1/4 fraction is called a 2^{k-2} design, a 1/8 fraction is called a 2^{k-3} design, and so on (Montgomery and Runger, 2003).

Our study involved the examination of the following six factors; Temperature (A), Closure Stress (B), Proppant Concentration (C), Polymer Loading (D), Clean up Flow Rate (E) and use of Breaker (F) to measure the major impact over the final fracture conductivity, therefore we considered using a 2^{k-3} fractional factorial design, where k=6. Since there are six main factors our primarily interest is to identify the main effect of each one of them, but at the same time it was our goal to obtain some information about the aliases or two-factor interactions. We initially designed a table consisting of 8 runs. We knew that with this design, the main effects were aliased with higher order interactions. Therefore, a second set of experiments were planned to make another 8 experimental runs. The combination of the first and second experimental runs (16 in total) enables us to isolate the relative effect of the main factors compared to each other. This type of design allows us to reduce the number of runs to 16 experiments that were then performed in two series of 8 experiments as opposed to 2^6 (64 experiments). The series of experiments and analysis of the design are presented in Tables 2.3 and 2.4 where the minus number indicates that the low level of that parameter is been investigated and the positive number indicates that the high level is been investigated.

Table 2.3 First schedule of fractional factorial design experiments

Experiment #	N2 rate, A (liter/min)	Temperature, B (°F)	Polymer loading, C (lb/1000gal)	Presence of Breaker, D	Closure Stress, E (psi)	Proppant Loading, F (ppg)
1	-1	-1	-1	-1	1	1
2	-1	-1	1	1	-1	-1
3	-1	1	-1	1	-1	1
4	-1	1	1	-1	1	-1
5	1	-1	-1	1	1	-1
6	1	-1	1	-1	-1	1
7	1	1	-1	-1	-1	-1
8	1	1	1	1	1	1

Table 2.4 Second schedule of fractional factorial design experiments

Experiment #	N2 rate, A (liter/min)	Temperature, B (°F)	Polymer loading, C (lb/1000gal)	Presence of breaker, D	Closure Stress, E (psi)	Proppant Loading, F (ppg)
1	1	1	1	1	-1	-1
2	1	1	-1	-1	1	1
3	1	-1	1	-1	1	-1
4	1	-1	-1	1	-1	1
5	-1	1	1	-1	-1	1
6	-1	1	-1	1	1	-1
7	-1	-1	1	1	1	1
8	-1	-1	-1	-1	-1	-1

Based on the first analysis, we see that the main effect and several 2nd order interactions are aliased or co-founded as is illustrated by Eq. 2.3. Notice that we have ignored effects of order 3 and higher based on the hierarchical ordering principle.

$$l_A = A + CF + DE$$

$$l_B = B + CE + DF$$

$$l_C = C + AF + BE$$

$$l_D = D + AE + BF$$

$$l_E = E + BC + AD$$

$$l_F = F + AC + BD \qquad \text{Eq. 2.3}$$

Once the first analysis was performed we proceeded and ran the second schedule. For the second set of experiments, the main and 2nd order interaction effects are still co-founded. We have also ignored the effects of order 3 and higher based on the hierarchical ordering principle.

$$l_A' = A - CF - DE$$

$$l_B' = B - CE - DF$$

$$l_C' = C - AF - BE$$

$$l_D' = D - AE - BF$$

$$l_E' = E - BC - AD$$

$$l_F' = F - AC - BD \qquad \text{Eq. 2.4}$$

By combining the effects estimated from the second set of experiments fraction with the effects estimated from the first set of experiments, we can isolate and uniquely determine the main effects and also estimate the effect of combined interactions. Table 2.5 shows how these factors can be calculated:

Table 2.5 Calculation of isolated factor and aliases factors

$From\ \frac{1}{2}(l_i + l_i')$	$From\ \frac{1}{2}(l_i - l_i')$
A	CF + DE
B	CE + DF
C	AF + BE
D	AE + BF
E	BC + AD
F	AC + BD

2.5 Experimental Conditions

This research aims to better represent reservoir conditions over the final value of fracture conductivity. It has been reported by Holditch (2006) that a tight gas reservoir can be found at deep or shallow depths, high-pressure or low-pressure, low temperature or high temperature, blanket or lenticular, homogeneous or naturally fracture, and can contain a single layer or multiple layers. The optimum stimulation treatment can only be achieved when the treatment is prepared taking into consideration all of the above characteristics of the reservoir.

During the realization of this research important factors such as closure stress, temperature, proppant loading are going to be studied and then analyzed. Other parameters such as polymer loading, the use of breaker, and the variation on the clean-up flow rate are going to be used during the realization of the experiments. The results and analysis of these experiments parameters can be found in the thesis of Juan Carlos Correa (2010).

This large number of parameters involve a large number of experiments, in order to reduce the number of experiments, by using the application of an experimental design technique known as Fractional Factorial Design (Montgomery and Runger, 2003; Myers and Montgomery, 2002) was used. The use of this technique allows researchers to reduce the number of experiments necessary to achieve the main objective in this investigation.

2.5.1 Fracture Fluid Composition

A fracturing fluid composition was provided by a service company for this experiment. The fracturing fluid was selected by the operator to simulate realistic gel used during a hydraulic fracturing treatment on tight sand reservoirs. Guar polymer was used as a base gel for this experiment. All experiments are conducted at room temperature during the fluid preparation.

The composition of the fracturing fluids used for the series of experiments is shown in Table 2.6 below:

Table 2.6 Main components of fracturing fluid

Chemical	Concentration
Guar, lb/Mgal	10-30
Hydration Buffer to pH	6.5
Buffer #2 to pH	10.0
Breaker, gal/Mgal (if used)	10.0
Breaker activator, gal/Mgal (if used)	1.0
Borate Crosslinker, gal Mgal	0.9
Crosslinker accelerator, gal/Mgal	0.2

The components for the selected fracturing fluid are as follows:

1. Guar: Dry polymer guar is used to form a viscous base gel fluid.
2. Buffers: Liquid weak acid and liquid carbonate are used to control pH, which is important for polymer hydration rate and crosslinking rate.
3. Breaker: The purpose of breaker is to reduce the viscosity of the polymer solution and provide rapid fluid clean up.
4. Breaker activator: Another type of oxidizer breaker is used to activate breaker for low temperature environment.
5. Crosslinker: To increase gel viscosity and give better proppant transport capability, borate crosslinker was used for this experiment.
6. Crosslink accelerator: To accelerate the crosslink time, a crosslink accelerator is used for this experiment because the fluids are mixed at room temperature.

2.5.2 Proppant Size and Loading

The proppant was provided by ***Carbo Ceramic***. It is a low weight ceramic proppant with 30-50 mesh size. A 30-50 mesh size proppant is considered a commonly used proppant in hydraulic fracture treatments in Texas and the low weight of this proppant in particular allows it to work with a low polymer concentration and with low viscosity fluid. The proppant was placed dynamically into the conductivity cell using of a centrifugal pump. The proppant loading of interest for this project are 0.5 ppg and 2 ppg.

2.5.3 Temperature

The temperature is one of the main factors of interest in this investigation. Temperature controls the breaking time of the gel, and also affects the mechanical properties of the proppant. In order to recreate the reservoir conditions during the realization of this research, the temperature in the conductivity cell is going to be controlled by a heating jacket that keeps the cell at a constant temperature during the entire experiment. The tubing used to connect the centrifugal pump with the conductivity cell is also preheated using a heating tape. This allows the gel to reach its final crosslinked point.

2.5.4 Clean Up Flow Rate

Wet nitrogen was use in these experiments to simulate gas production from the fracture into the wellbore. A flow rate for the laboratory setup was calculated to simulate a field production rate of 2.04 MMscf/d and 12.28 MMscf/d using the values from Table 2.7 and the equations below.

Table 2.7 Comparison of laboratory and field conditions

	Laboratory Conditions	Reservoir Conditions
Fracture height (h)	1.6 in.	100 ft
Fracture width (w)	0.04	0.25 in.
Temperature (T)	150 $^{\circ}$F – 250 $^{\circ}$F	250 $^{\circ}$F
Flowing pressure (p_{wf})	50 psi	1000 psi

We can start calculating the flux and the production rate in the experiment by:

$$q_{sc}=3\text{slm}\left(0.0353\frac{\text{ft}^3}{\text{l}}\right)=0.1059\frac{\text{SCF}}{\text{min}}$$ Eq. 2.5

$$B_g=\frac{ZT/p}{Z_{sc}T_{sc}/p_{sc}}$$ Eq. 2.6

$$B_g=\frac{(1)(150+460)\ /50}{(1)(60+460)/14.7}=0.3448\frac{\text{ft}^3}{\text{SCF}}$$

$$q=B_g q_{sc}$$ Eq. 2.7

$$q=0.1059\frac{\text{SCF}}{\text{min}}0.3448\frac{\text{ft}^2}{\text{SCF}}=0.0365\frac{\text{ft}^3}{\text{min}}$$

$v_{lab}=\frac{q}{A}$; where A= w*h, this equation can be written as:

$$v_{lab}=\frac{q}{w\,h}$$ Eq. 2.8

$$v_{lab}=\frac{0.0365\frac{\text{ft}^3}{\text{min}}}{(1.6\text{in})(0.04)\text{in}}144\frac{\text{in}^2}{\text{ft}^3}=82.125\,\text{ft/min}$$

Gas flux at laboratory condition is 82.13 ft/min.

Under reservoir conditions:

$$B_g = \frac{(1)(250+460)\ /1000}{(1)(60+460)/14.7} = 0.0201\ \frac{\text{ft}^3}{\text{SCF}}$$

$$q = v_{frac}\, A \qquad \text{Eq. 2.9}$$

$$A = 82.13\ \frac{\text{ft}}{\text{min}}\ 100\ \text{ft}\ 0.25\text{in}\ \frac{1\text{ft}}{12\text{in}} = 171.104\ \frac{\text{ft}^3}{\text{min}}$$

$$q_{sc} = \frac{q}{B_g} \qquad \text{Eq. 2.10}$$

$$q_{sc} = \frac{171.104\ \text{ft}^3/\text{min}}{0.0201\ \text{ft}^3/\text{SCF}} = 8525.36\ \frac{\text{SCF}}{\text{min}}$$

$$q_{sc} = 8525.36\ \frac{\text{scf}}{\text{min}}\ \frac{(24)(60)}{1}\ \frac{\text{min}}{\text{day}} = 12.28\ \frac{\text{MMSCF}}{\text{Day}}\ \text{(1 Wing)}$$

where q is the injection rate, Bg is the formation volume factor, A is area, T is temperature, p is pressure, w is fracture width, and h is fracture height.

2.5.5 Closure Stress

Closure stress conditions were implemented in these experiments to simulate the fracture shut-in typically encounter during a fracture treatment. The closure stress was varied between 2000 psi to 6000 psi to simulate a deeper tight sand reservoir. Each stress was held during the entire time while conductivity was measured and recorded. This further contributed to the understanding of the proppant pack degradation in the field. Table 2.8 present a summary of the parameters to be investigated and analyzed during this research**.**

Table 2.8 Parameters to be analyzed

Parameter	**Levels**
Nitrogen Flow Rate	0.5 slm/ 3 slm
Polymer Loading	10 lbm/Mgal/ 30 lbmMgal
Breaker	With breaker/ Without breaker
Temperature	150 $^{\circ}$F/ 250 $^{\circ}$F
Proppant Loading	0.5 ppg/ 2 ppg
Closure Stress	2000 psi/ 6000 psi

CHAPTER III

RESULTS AND DISCUSSION

We conducted a series of experiments using Ohio Scioto sandstone with different proppant concentrations at different temperatures and different closure stresses. For each rock tested, wet nitrogen was flowed through the fracture at two different flow rates. To evaluate the consistency of our experiment results and experiment procedures, some of the experiments were repeated within the same conditions.

3.1 Calibration Test

Before proceeding with the experiments needed to reach the objectives of this research we performed a number of experiments to validate that the experiments are consistent with results from previous research (Marpaung et al., 2008). These first set of experiments were performed with the objective to calibrate the new equipments and to validate the deliverability of our new series of experiments. Table 3.1 shows the parameters of this experiment; Fig. 3.1 shows the performance of conductivity as a function of time and Fig. 3.2 shows a picture of the sand placed on the face of the cores. As was explained in the previous studies the conductivity increases progressively during a period of time after conductivity test begins, this is known as the “clean up time”. The conductivity will there reaches its maximum value after several hours. This was observed in a similar way as it was reported from the previous study. Additional data can be found in the appendix in Fig. A.2 and Table A.1.

Table 3.1 Dynamic fracture conductivity test conditions

Proppant loading	2	ppg
Polymer loading	30	lbm/Mgal
Temperature	150	$^{\circ}$F
Gas flow rate	1	L/min
Use of Breaker	Yes	
Closure Stress	2000	psi
Proppant Concentration	0.46	lbm/sq ft

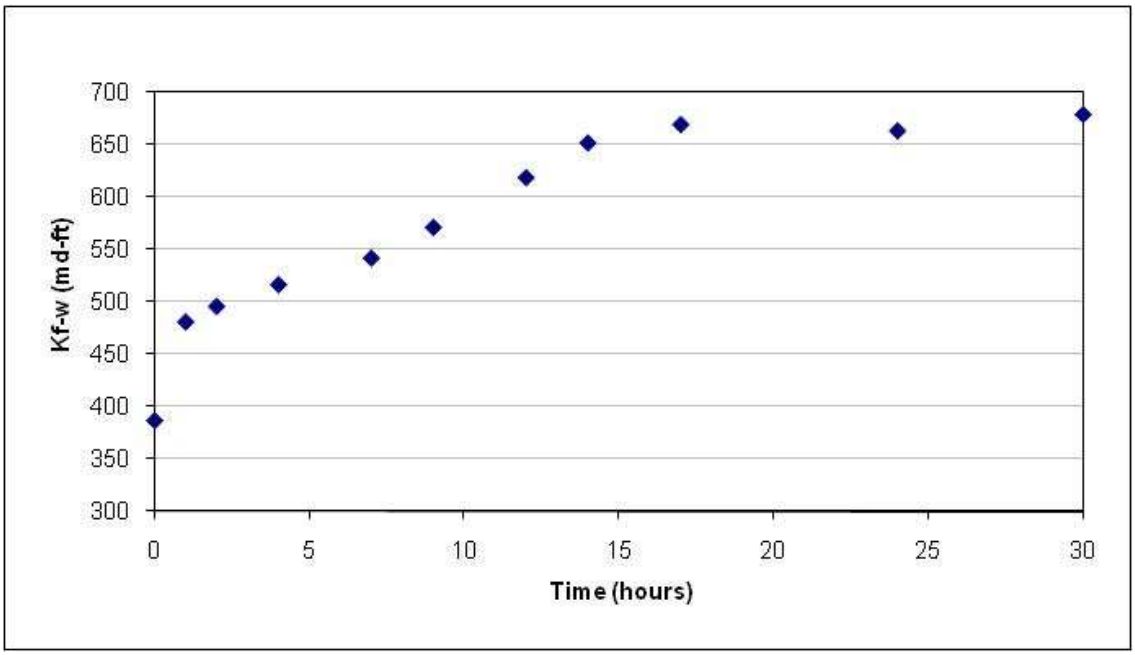

Fig. 3.1 Fracture conductivity calculated from Forcheimer's equation

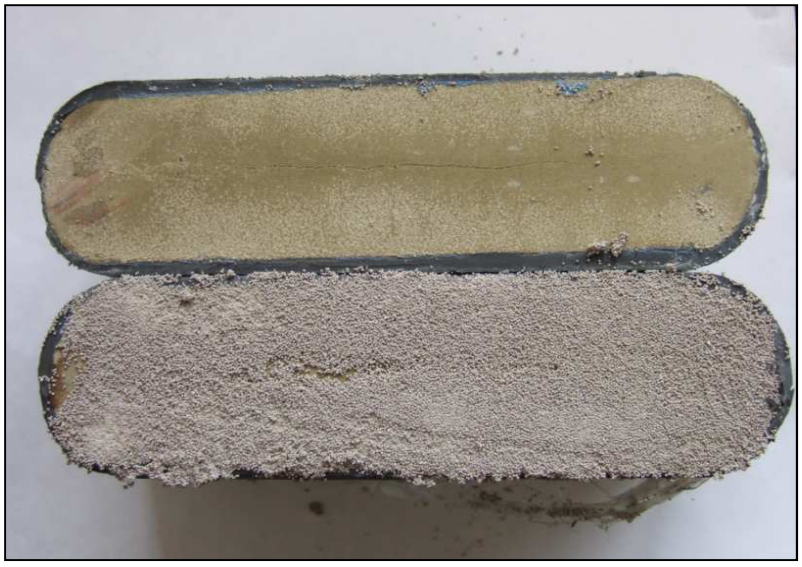

Fig. 3.2 Proppant placement over the core surface

3.2 Fractional Factorial Design Results

The first set of fractional factorial design experiments are summarized in Table 3.2. The second group of experiments is presented in Table 3.3 the combination of these two sets of experiments allowed us to identify the estimated effect of each factor and the effect of combined aliases. The conductivity values of each experiment are discussed and presented as well as a comprehensive interpretation in this chapter.

Table 3.2 Test conditions and result for the first schedule of fractional factorial design experiments

Experiment #	N2 rate, A (liter/ min)	Temp., B (°F)	Polymer loading, C (lbm/ 1000gal)	Presence of Breaker , D	Closure Stress, E (psi)	Proppant loading, F (ppa)	Dynamic fracture conductivity (md-ft)
1	0.5	150	10	No	6000	2	570.06
2	0.5	150	30	Yes	2000	0.5	1647.48
3	0.5	250	10	Yes	2000	2	2011.77
4	0.5	250	30	No	6000	0.5	15.2
5	3	150	10	Yes	6000	0.5	960
6	3	150	30	No	2000	2	1060.87
7	3	250	10	No	2000	0.5	1098.58
8	3	250	30	Yes	6000	2	155.87

Table 3.3 Test conditions and result for the second schedule of fractional factorial design experiments

Experiment #	N2 rate, A (liter/ min)	Temp., B (○F)	Polymer loading, C (lbm/ 1000gal)	Presence of breaker, D	Closure Stress, E (psi)	Proppant loading, F (ppa)	Dynamic fracture conductivity (md-ft)
1	3	250	10	No	6000	2	118
2	3	150	30	No	6000	0.5	16
3	0.5	150	10	No	2000	0.5	2484.50
4	0.5	250	10	Yes	6000	0.5	476.03
5	0.5	250	30	No	2000	2	959.00
6	3	250	30	Yes	2000	0.5	688.00
7	0.5	150	30	Yes	6000	2	410.25
8	3	150	10	Yes	2000	2	1477.00

Results from the combined interaction of the main factors and the aliases combinations from the first and second schedule are presented in Table 3.4 and 3. 5. To judge the variables influencing fracturing conductivity, we combined the experiment results obtained from both schedules. Table 3.6 presents the results for each independent factor and the results for the aliases combined factor. Following the hierarchical ordering principle, the higher order effects were considered insignificant and were not taken into consideration for this study.

Table 3.4 Results of the aliases combinations for the first schedule of experiments

	Factor	Aliases Combinations	Aliases Effects
A	N2 FLOW RATE (L/min)	A+CF+DE	-261.4
B	TEMPERATURE (F)	B+CE+DF	-258.09
C	POLYMER LOADING (lb/Mgal)	C+AF+BE	-421.41
D	BREAKER USE	D+AE+BF	526.44
E	CLOSURE STRESS (psi)	E+BC+AD	-1048.23
F	PROPPANT LOADING. (ppg)	F+AC+BD	0.49

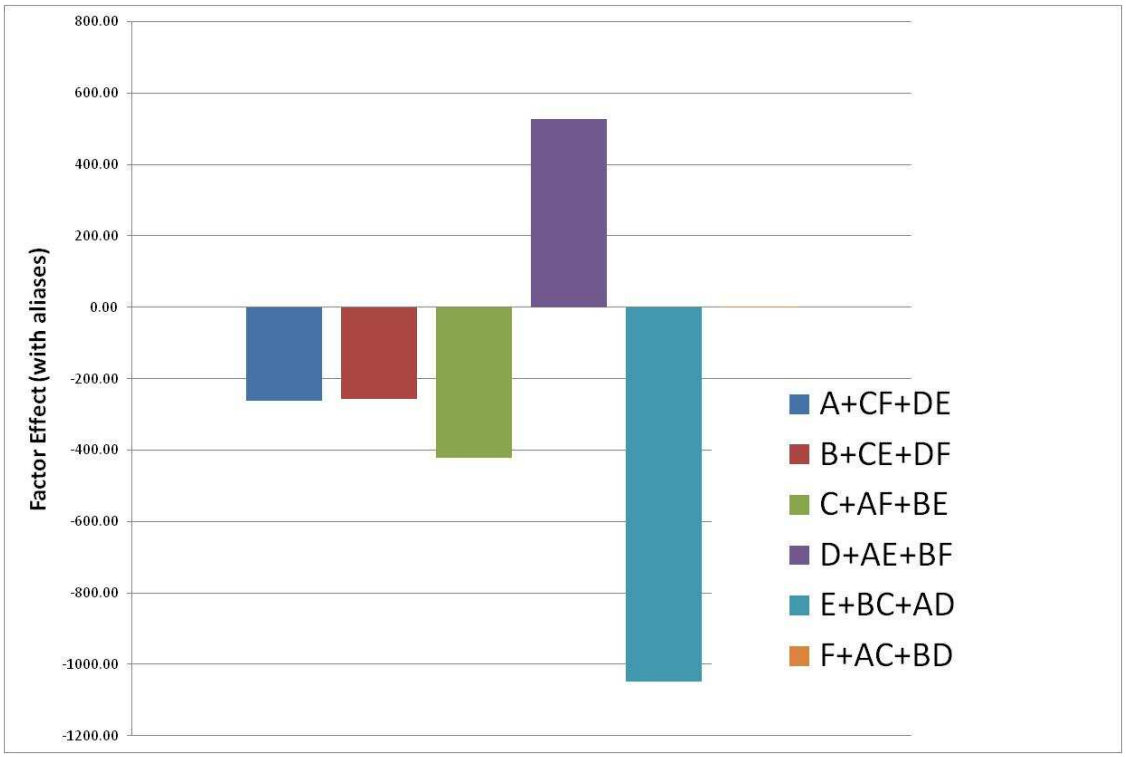

Fig. 3.3 Bar chart representation of the aliases factor effect from the first schedule of experiments

Table 3.5 Results of the aliases combinations for the second schedule of experiments

	Factor	Alias Combinations	Aliases Effects
A	N2 FLOW RATE (L/min)	A-CF-DE	-713.18
B	TEMPERATURE (F)	B-CE-DF	-742.17
C	POLYMER LOADING (lb/Mgal)	C-AF-BE	-415.09
D	BREAKER USE	D-AE-BF	73.93
E	CLOSURE STRESS (psi)	E-BC-AD	-941.57
F	PROPPANT LOADING. (ppg)	F-AC-BD	30.42

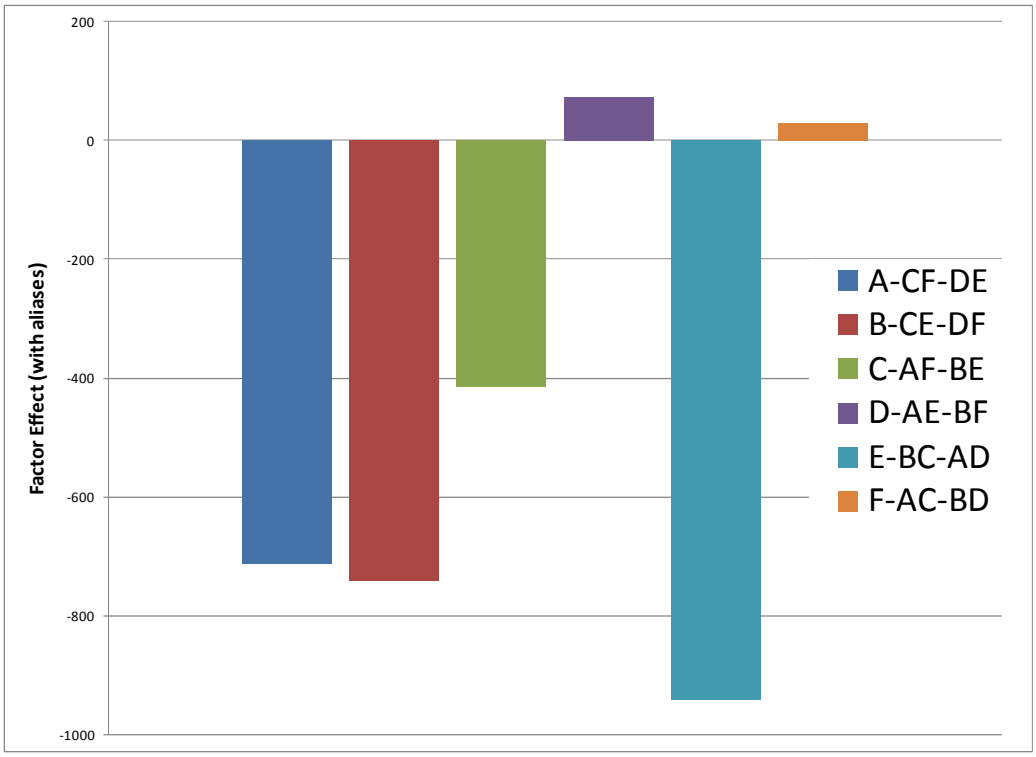

Fig. 3.4 Bar chart representation of the aliases factor effect from the second schedule of experiments

Table 3.6 Results for each independent factor and for the aliases factor

	Factor	Factor Effect (without aliases)	Aliases Combinations	Aliases Effects
B	TEMPERATURE (F)	-418.24	AF+BE	-3.16
E	CLOSURE STRESS (psi)	-994.90	BC+AD	-53.33
F	PROPPANT LOADING. (ppg)	15.45	AC+BD	-14.96

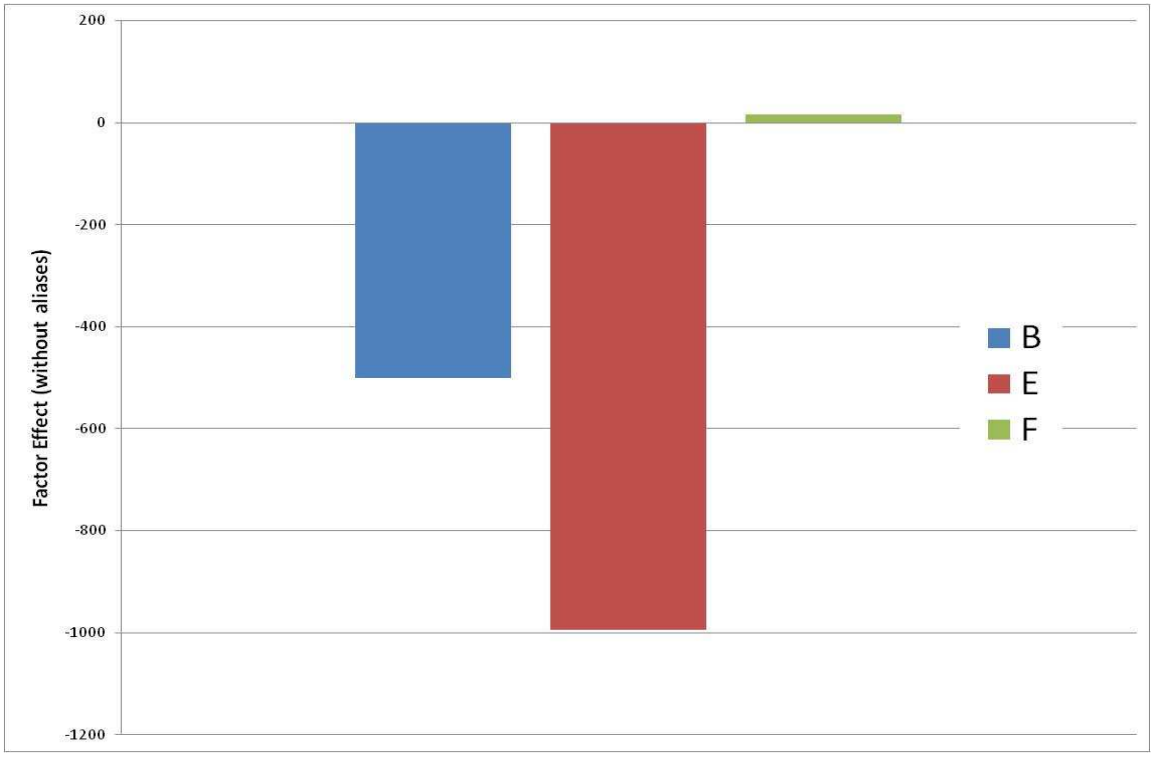

Fig. 3.5 Bar chart representation of the effect of isolated factors

From Fig. 3.3, 3.4, and 3.5 it is possible to identify the estimated responses of each parameter using this particular experimental design over the final conductivity. The negative sign in the evaluation means that the magnitude of the parameter had an inverse effect over the conductivity, meaning that if the magnitude of the parameter increases the final conductivity decreases. We must take into consideration that this experimental design process is just a first screening process and a first step in the development of a statistical model. However, further experiments are recommended to understand and identify the full effect of each parameter combination over the final conductivity and to develop a final and robust statistical model.

3.3 Effect of Proppant Loading over the Fracture Conductivity

After completing all the experiments necessary to perform the fractional factorial design analysis, the following interpretation can be derived from the comparison of each experiment results. A major amount of proppant mixed with the gel resulted into a larger amount of proppant inside the fracture this help to maintain a greater width and prevent the crushing and fine generation from proppant. However, to be able to carry a higher amount of proppant the gel needs to increase its viscosity in order to overcome the settling or deposition of the solids particles on its way to the conductivity cell. A raise in viscosity can be reached by increasing the polymer loading or increasing carefully the amount of crosslinker without over crosslinking the gel. The effect of these two factors was not analyzed during this research, but it has been reported to have a negative impact over the final conductivity (Kim and Losacano, 1985; Marpaung et al., 2008; Volk et al., 1983).

Fig. 3.6 shows the results of conductivity against closure stress for both cases of proppant loading. The trend on this figure indicates that at higher levels of proppant loading a higher conductivity was obtained. This figure helps to reinforce the concept that a major proppant loading provides a higher conductivity. Low values of conductivity reported on this figure correspond to those experiments where no breaker was used preventing a full clean up of the proppant pack.

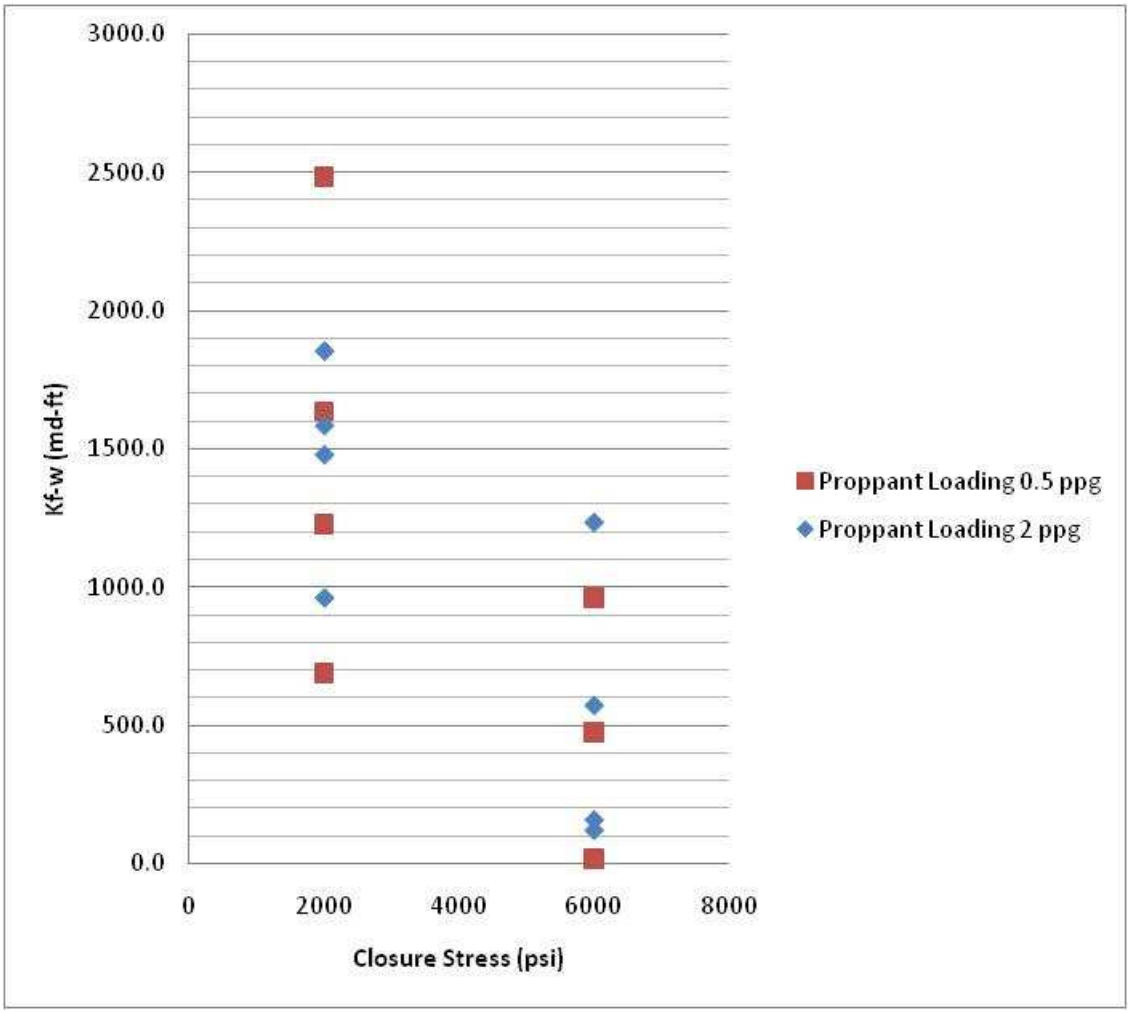

Fig. 3.6 Conductivity result as a function of closure stress for both levels of proppant loading

Regarding proppant distribution, interesting results were obtained. It has been estimated that a larger amount of proppant is capable of maintain the fracture open after closure stress is applied. However, during this investigation interesting results were obtained when a low level of proppant loading was studied. Fig. 3.7 presents a comparison between the fracture conductivity response for a case where a homogeneously distributed proppant was placed and a proppant pack with a channel in the middle. The channel in the middle of the proppant bed creates a high path for gas to flow through the conductivity cell, resulting in a fracture conductivity almost 4 times higher. Fig. 3.8 and 3.9 show the proppant placement for each one of the cases respectively.

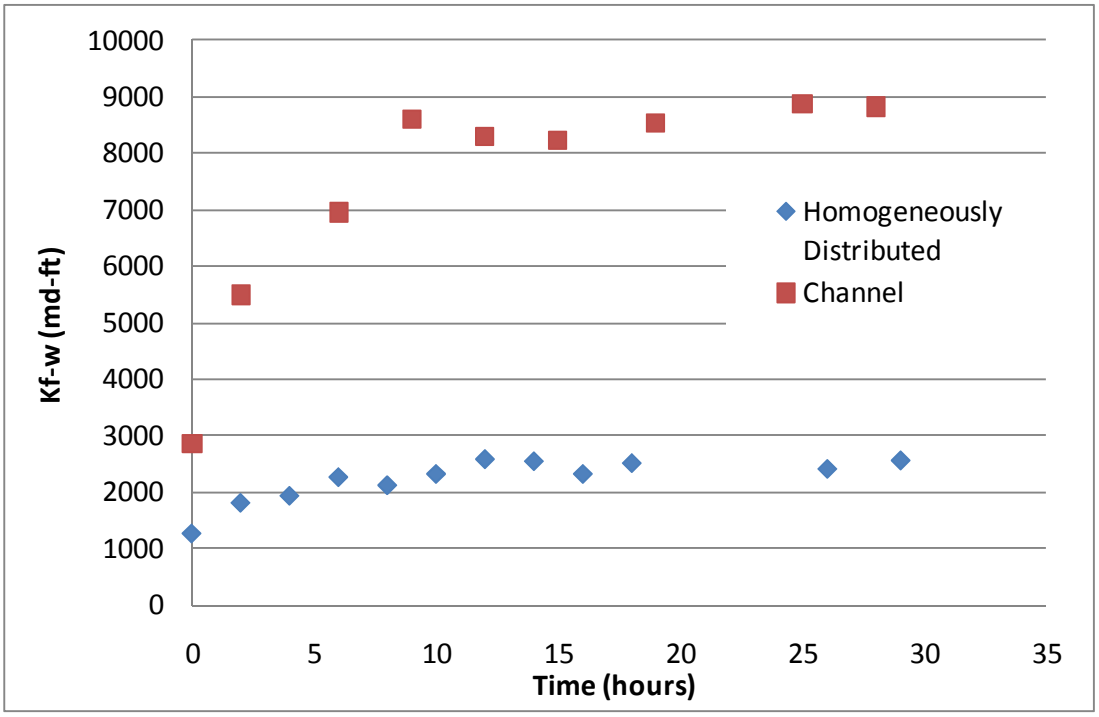

Fig. 3.7 Conductivity of a homogeneously distributed proppant pack compared with conductivity of a proppant pack with a channel in the middle

Fig. 3.8 Homogeneously distributed proppant placement

Fig. 3.9 Proppant placement with a channel in the middle

A similar result was observed in another case where low proppant loading was used. However, in this case the high conductivity was created due to void spaces in the proppant pack. In a similar way these void spaces creates high flow lanes within the proppant pack. Fig. 3.10 presents a picture taken after an experiment where low levels of closure stress, proppant loading and temperature were used and void spaces were formed.

Fig. 3.10 Proppant placement with void spaces

3.4 Effect of Temperature over the Fracture Conductivity

Temperature controls the breaking time of the gel and also affects the mechanical properties of the proppant. The conductivity cell is shut in at a constant temperature for a period of time of 10 hours. This period of time was selected due to the fact that polymer is designed to break in 5 hours and from positive results in previous researches. The shut in time is the same for both temperature levels. Fig. 3.11 displays all of the final conductivity values for each test at two different temperature levels where the experiments are then grouped by similarities in design parameters.

Notice the experiments with a high level of temperature (250 $^{\circ}$F) tended to result in a lower conductivity. It is consider that the behavior of the conductivity is produced by a loss of fluid integrity because the period of shut in was too long for the cases where a higher temperature was evaluated. These conditions degraded the polymer to the point where broken and unbroken polymer dried up creating obstructions in the proppant pack.

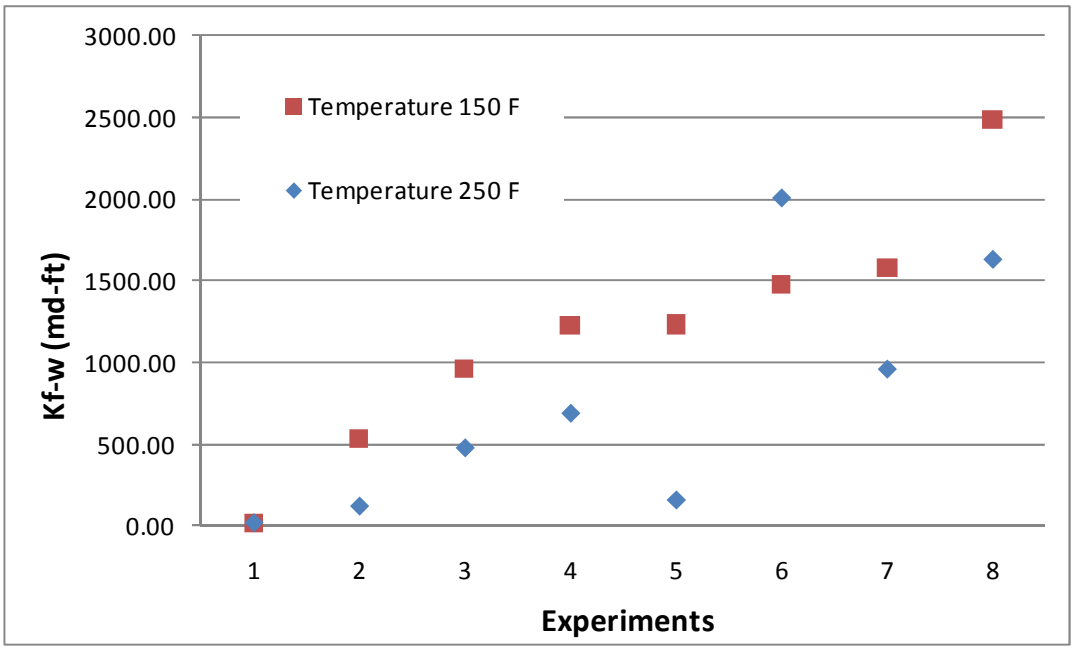

Fig. 3.11 Final conductivity values for temperatures of 150 F and 250 F

Similar results are observed when high temperatures and high closure stress are combined; Fig. 3.12 presents the results of the conductivity under a constant closure stress for both temperatures. Observing this figure it is possible to detect an interaction between these two parameters that reduce significantly the conductivity of the proppant pack, it is recommended for future research to analyze in more detail the interaction of these two factors and the shut in time over the final conductivity to design new experimental guidelines.

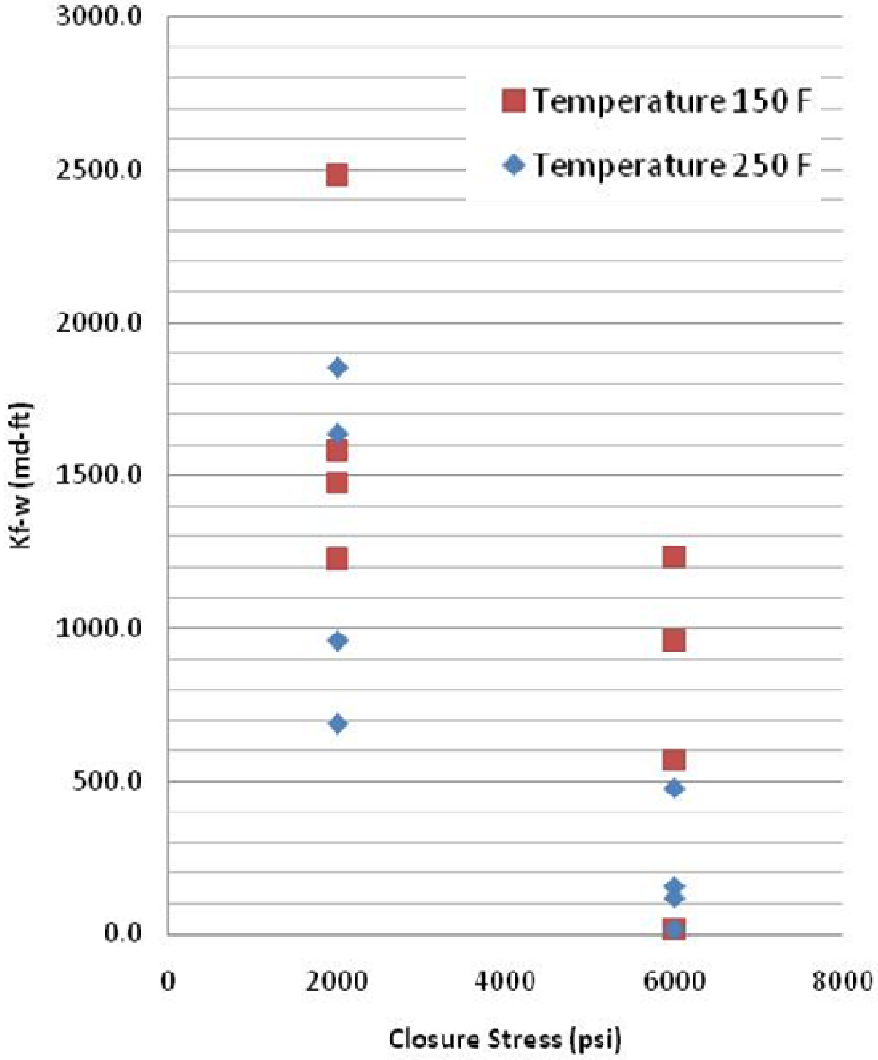

Fig. 3.12 Conductivity values against closure stress for both levels of temperature

3.5 Effect of Closure Stress over the Fracture Conductivity

To summarize the results of each test it is important to analyze the final conductivity at each level of closure stress. Fig. 3.13 and 3.14 present the conductivity at different closure stresses of 2000 psi and 6000 psi and different proppant loading of 0.5 ppg and 2 ppg at a constant temperature. Experiments where low closure stress (2000 psi) was used reported both a higher conductivity and lower degradation of the proppant pack. The negative effect of the closure stress is more noticeable on those experiments were a low level of proppant was used. As closure stress increases the fracture conductivity decreases. This effect produces a smaller fracture width and higher degradation of the proppant pack.

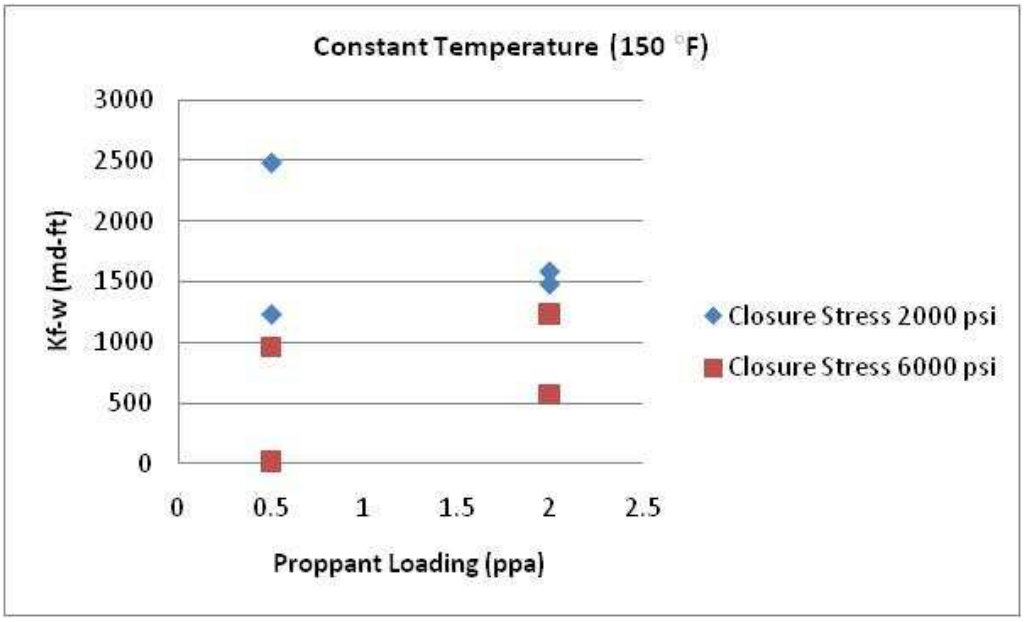

Fig. 3.13 Comparison of conductivity results at constant temperature (150 °F)

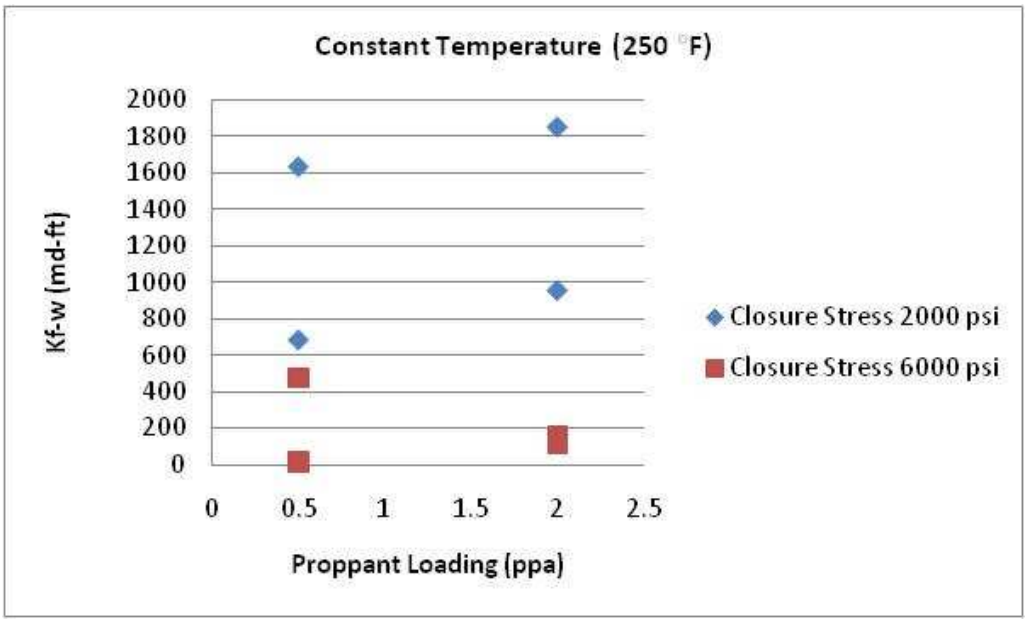

Fig. 3.14 Comparison of conductivity results at constant temperature (250 °F)

Some additional results were obtained under 250 °F and 6000 psi. In these experiments the unbroken polymer dried up creating a scale of proppant, and fines, therefore, resulting in a significant reduction on fracture conductivity. Fig. 3.15 and 3.16 show the descriptive images of those types of experiments.

Fig. 3.15 Scale formed by proppant, fines, and dried polymer over the core surface

Fig. 3.16 Enlargement of the scale formed by proppant, fines, and dried polymer over the core surface

3.6 Rock Hardness and Embedment

Proppant embedment is a serious problem that can reduce fracture width and conductivity. Under bottom-hole stress conditions proppant tends to embed into the fracture surface, and create fines. Embedment Pressure tests (Howard and Fast, 1970) were carried out during this project and the results of these tests are presented in Table 3.7. The range of embedment stress has been reported between 13,000 psi to 527,000 psi by Howard and Fast (1970). For the Scioto Ohio sandstone used in this research the average value of embedment stress was calculated as 244,760 psi, meaning that the Scioto Ohio sandstone is in a range of middle to high embedment stress rock.

During our experiments we noticed the presence of proppant embedment on the surface of the cores. The embedment is more appreciable in those cases where higher closure stress was applied. However, after we analyzed the results from the embedment test and evaluated the surface of the cores it was concluded that the use of lightweight ceramic proppant provides a low indentation on the rock surface therefore, reducing the risk of fine production from the rock surface. Fig. 3.17 presents the surface of the core after the proppant has been removed.

Table 3.7 Embedment pressure results

Points	Sre, psi
1	226,762.94
2	226,762.94
3	251,958.83
4	25,195.88
5	264,556.77
6	251,958.83
7	277,154.71
8	302,350.59
9	264,556.77
10	251,958.83
11	302,350.59
12	251,958.83
13	264,556.77
14	264,556.77

Fig. 3.17 Common indentation marks over cores surface after proppant was removed

3.7 Sieve Analyses on Proppant after Conductivity Test

This research was carried out using lightweight ceramic proppant. To further study the proppant behavior a sieve analysis of each proppant sample was done after each one of the experiments were completed and reported in section 3.2. The analysis was done before and after the conductivity test for comparison purposes. The proppant samples can then be checked to quantify the amount of crushed material that occurred when subjected to a high stress and high temperatures.

The results of a sieve analysis of a sample after the conductivity test was performed can be found in Fig. 3.18**.** In this figure it is possible to observe the low degradation and well performance of the proppant under a closure stress of 2000 psi and temperature of 150 $^{\circ}$F. Fig. 3.19 presents the results of two samples after the conductivity test was carried out under high temperature and high closure stress conditions. In this case sample “A” presented a 20% of the total weight of the proppant removed from the surface of the rock passing the 70 micron sieve. This amount of crushed proppant is responsible for a reduction of 13% on conductivity when compared with sample “B” tested under the same conditions.

A greater amount of crushed material occurred as a result of irregular accumulation of proppant over the surface of the rock. When an uneven distribution occurs, more pressure is applied on a specific area of the proppant pack, this create more fines when compared with a case where the proppant layer is evenly distributed and the pressure is equally applied all over the proppant pack.

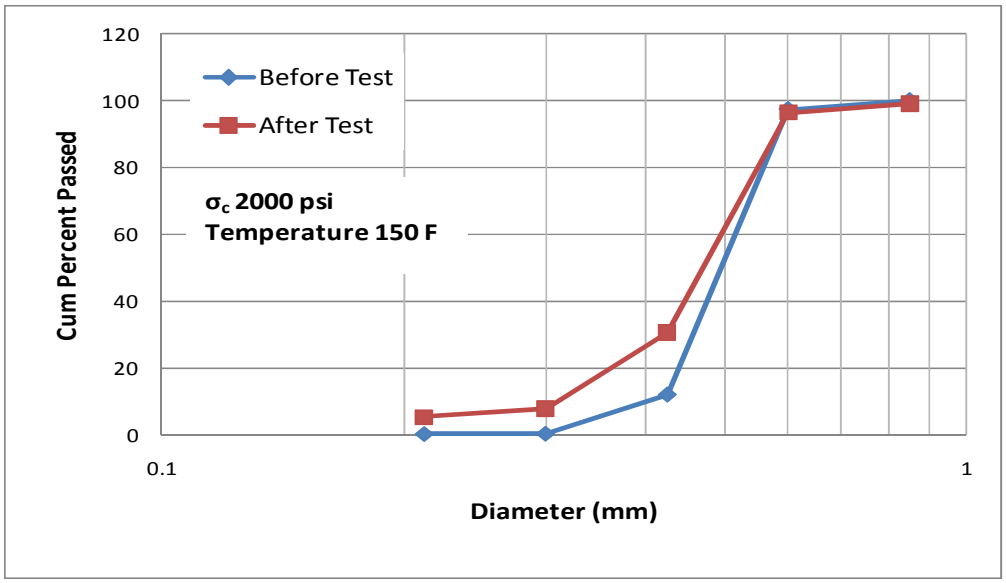

Fig. 3.18 Sieve analyses on proppant before and after test under low pressure and low temperature

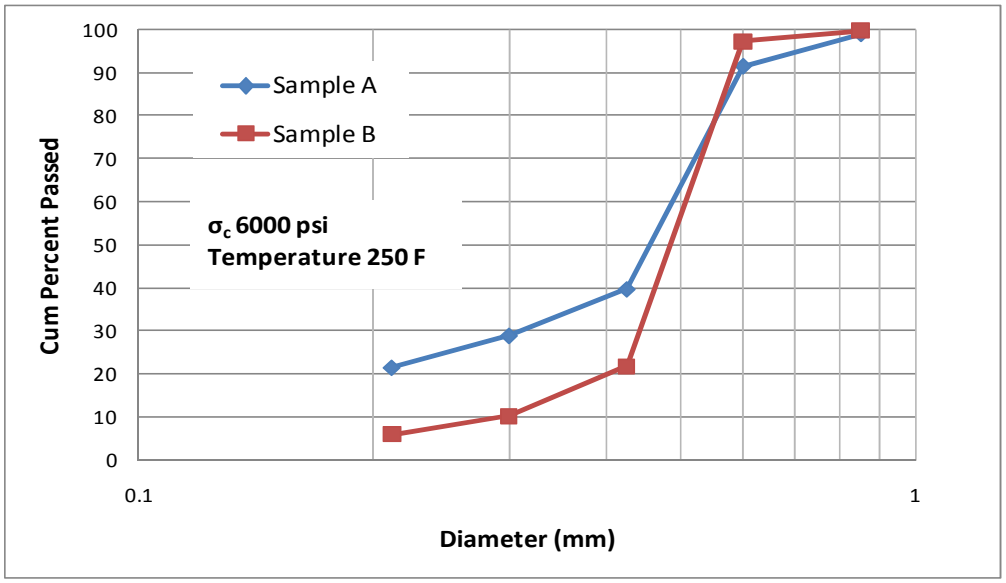

Fig. 3.19 Sieve analyses on proppant after test under high closure stress and high temperature

For those experiments were breaker was not used, it was common to identify masses of crushed proppant compacted with dry gel. These masses were found on the first sieve (20 micron) after the sieve analysis is performed. Fig. 3.20 shows a typical result of the sieve analysis for these cases. Additional sieve analysis can be found in appendix A.3.

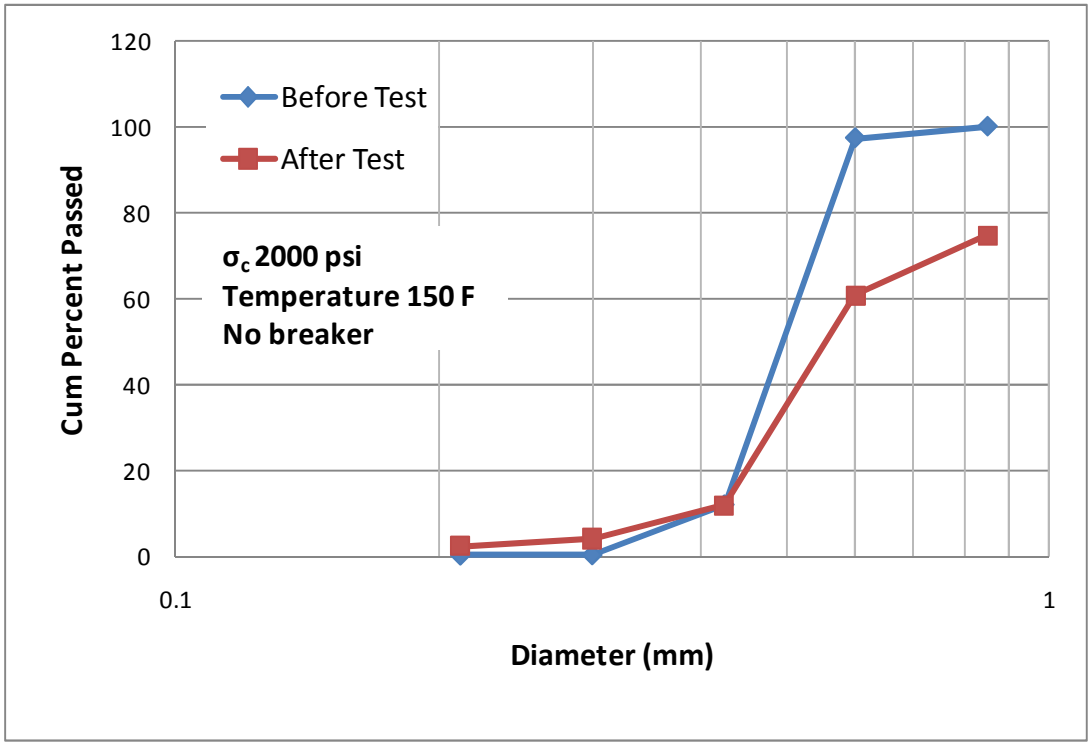

Fig. 3.20 Sieve analyses on proppant before and after the test where no breaker was used

3.8 Lessons Learned

3.8.1 Mixing System

The original design of the experiments recommended mixing both the base gel and the slurry using the mixing tank. This mixing process works well for the base gel. However, for the slurry the creation of a vortex is only obtained if the mixer runs at high speed. When using the mixing tank at high speed a large amount of air is trapped in the gel, creating a foamy surface. To overcome this problem a 5 gallons bucket and a paddle mixer were used to mix the gel creating a vortex without the formation of foam. The presence of a vortex during the mixing process is important to identify the moment when the gel is partially consslinked.

3.8.2 Crosslinker Injection

The original procedure for the crosslinker injection stated that the injection of the crosslinker should be done using a metering pump on the inlet of the multi stages centrifugal pump. We found this procedure inadequate since the calculation of a pumping rate to fully mix the crosslinker with the gel was difficult to achieve. Additionally, for those cases where low polymer loading was used the gel was unable to reach enough viscosity to carry the proppant into the pump. We recommend, adding the crosslinker and the crosslinker accelerator into the 5 gallons bucket and monitoring the behavior of the vortex until it closes.

3.8.3 Dead Volumes

Dead volumes or void volumes in the pipe between the mixing tank and the multi stage centrifugal pump provide the perfect spaces for proppant to settle down before it reaches the centrifugal pump, making difficult to maintain a homogeneous proppant concentration in the slurry. We recommend reducing the amount of dead volume or voiding spaces reducing the number between the tanks and the multistage centrifugal pump.

3.8.4 Pressure Sensors

The use of new pressure sensors provided a superior accuracy for measuring low pressure, while been able to withstand the abuse of laboratory testing. Fig. 3.21 shows the new pressure sensors and diaphragm used on this project. This type of sensor allows the use of different diaphragms that range from 0.08 psi to 3200 psi depending on the requirements of the experiment.

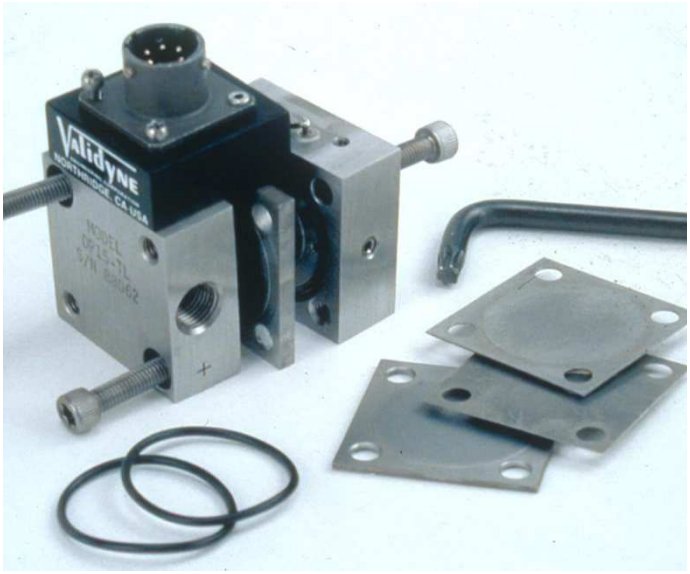

Fig. 3.21 New high accuracy pressure sensor Validyne, DP15

3.8.5 Heating Section

The original cylindrical heaters used to heat up the fluid before it reaches the conductivity cell were replaced by heating tape. Since the inner radius of the ceramic heater was much bigger than the outer radius of the tubing used in the experimental apparatus, the ceramic heathers needed to be set at extremely high temperature in order to heat up the fluids to 150 F. The heating tape provides a more efficient way to heat up the fluids. Fig. 3.22 shows the current heating tape and cylindrical ceramic heaters from the previous apparatus design.

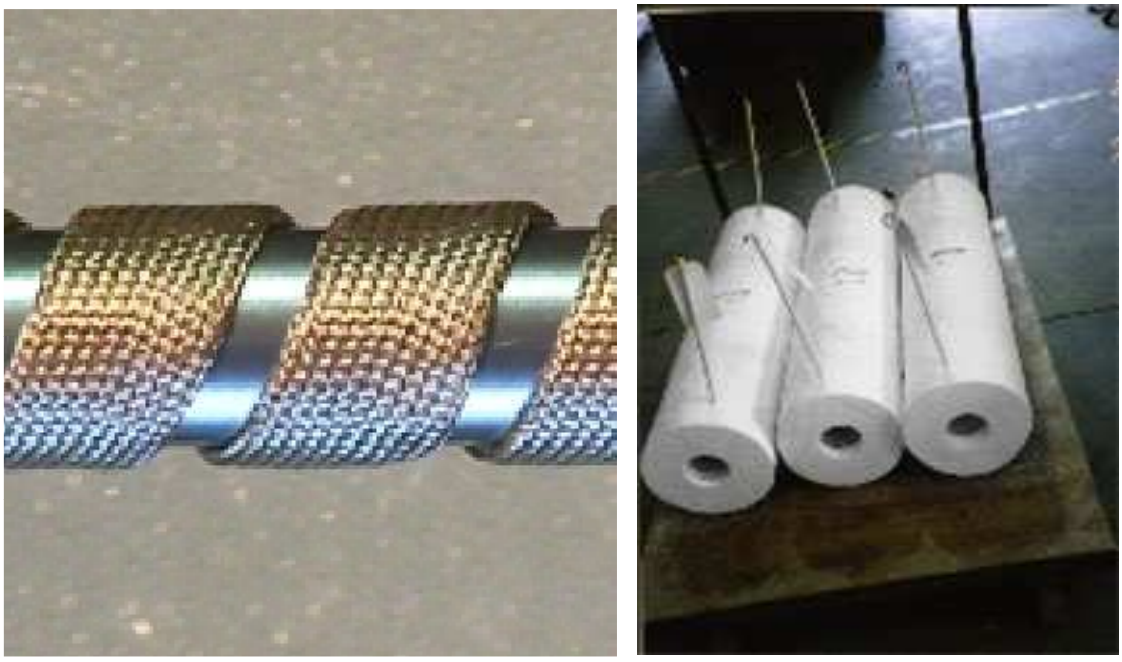

Fig. 3.22 New heating tape and old cylindrical ceramic heater

3.8.6 Accumulator and O-Rings

The conductivity cell uses two o-rings to prevent the flow of fluid or gasses between the walls of the cell and the cores. We recommend changing these o-rings every five experiments if the temperature used is around of 150 $^{\circ}$F and change it every two experiments if the temperature used is around 250 $^{\circ}$F. We observed that under higher temperatures the o-rings change shape and seals are disrupted allowing fluids to flow between the cell walls and the cores.

The accumulator was used to collect the proppant and to create back pressure in the system. This accumulator must be clean after every 5 experiment to remove the

proppant. We concluded that after five experiments the proppant accumulated will choke the inlet of the accumulator, blocking the entire flow in the system. Fig. 3.23 shows the accumulator and o-ring used in this project.

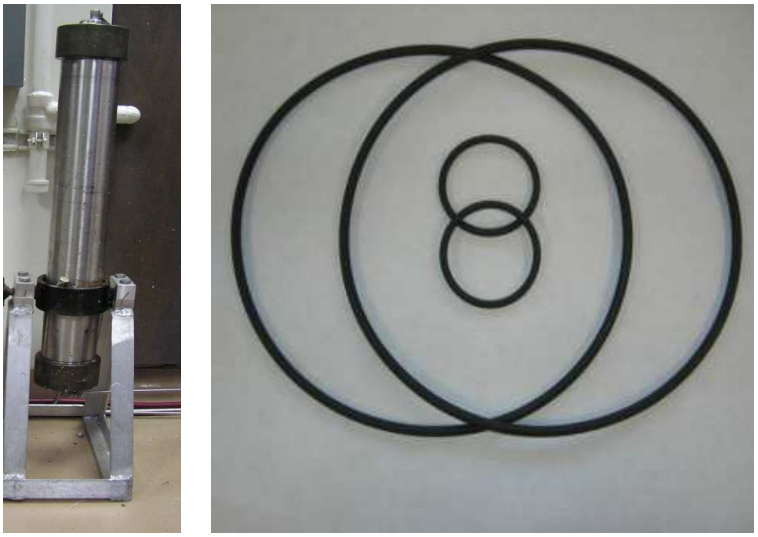

Fig. 3.23 Back pressure accumulator and sealing o-rings

CHAPTER IV

CONCLUSIONS AND RECOMMENDATIONS

4.1 Conclusions

Dynamic conductivity tests were conducted for up to 24 hours at different closure stresses, temperatures, and proppant concentrations. The behavior of the proppant and the effect of each one of the previously mentioned factors were measured. The following conclusions are made based on observations made in the study:

- An increment in closure stress has a major inverse impact over the final conductivity due to compaction and crushing of the proppant pack.

- Temperature influences the breaking capability of fracturing fluid and fracturing fluids properties. Experimental temperature around 250 $^{\circ}$F resulted in dried residual unbroken polymer in the fracture causing a reduction on the final conductivity.

- There is a distinct difference in performance when comparing a uniform distributed proppant pack and a proppant pack where channels or void spaces are present. Channels and void spaces on the proppant pack provide a higher conductivity due to the high permeability paths created in these cases.

- When analyzing the sieve analysis and comparing them to the conductivity tests, there is evidence of a loss of conductivity when the crushing increases. In the cases where no breaker was used the creation of scales is responsible for a large reduction in conductivity.

- A higher amount of crushed proppant can be expected when the settling of proppant is not evenly uniform over the rock surface.

- The Scioto Ohio sandstone used in this research has an average embedment pressure equal to 244,760 psi. resulting in a minor damage of the rock surface due to the embedment of light ceramic proppant.

- A reasonable and repeatable conductivity was measured using the set up apparatus with crosslinked gel. Different type of breakers with different fracture fluids could be used to compare different cleanup scenarios.

4.2 Recommendations

Dynamic hydraulic fracture tests and fracture conductivity were performed and analyzed during the realization of this project using equipment and conditions that resemble in more detail the field conditions.

The uses of Scioto sandstone during these experiments were used to simulate more closely the properties of reservoir rock. However, different proppants can be used to further expand the study and improve the outcomes of the experiments. Higher strength proppants such as bauxite could be used to study and see if there would be a smaller magnitude of degradation to the proppant pack under high pressure and high temperature. New approaches such as the employment of synthetic fibers in conjunction with low polymer concentration gel could be analyzed to investigate their impact over proppant transport and fracture clean up.

Additionally, rock properties such as the rock embedment strength and sieve analysis should be considered as standard part of the study for future projects with the purpose to quantify the rock and proppant responses and its effect on conductivity. Also the use of different breakers with the intention to evaluate the final amount of unbroken gel in the fracture could be considered.

We carefully quantified the fracture conductivity variation under different conditions to indentify the effect of various design parameters, while reducing the required number of experiments. However, additional experiments are recommended to provide a basis for a

better understanding of the impact of the remaining aliases over the fracture conductivity and to verify the possibility of developing a statistical model that could be used to predict dynamic fracture conductivity.

REFERENCES

API *RP 61. Recommended Practices for Evaluating Short-Term Proppant-Pack Conductivity*. first edition. 1989. Washington, DC: API.

Dewprashad, B.T., Weaver, J.D., Nguyen, P.D., Parker, M., and Blauch, M. 1999. Modifying the Proppant Surface to Enhance Fracture Conductivity. Paper SPE 50733 presented at the SPE International Symposium on Oilfield Chemistry, Houston, Texas, USA, 16-19 February doi:10.2118/50733-MS.

Flowers, J.R., Hupp, M.T., and Ryan, J.D. 2003. The Results of Increased Fracture Conductivity on Well Performance in a Mature East Texas Gas Field. Paper SPE 84307 presented at the SPE Annual Technical Conference and Exhibition, Denver, Colorado, USA, 5-8 October. doi:10.2118/84307-MS.

Holditch, S.A. 2006. Tight Gas Sands. *J Pet Technol* **58** (6): 86-93. SPE-103356-MS. doi:10.2118/103356-MS.

Howard, G.C. and Fast, C.R. 1970. *Hydraulic Fracturing*. Monograph Series, SPE, Richardson, Texas **2**: 60-71.

Kaufman, P.B., Anderson, R.W., Parker, M.A., Brannon, H.D., Neves, A.R. et al. 2007. Introducing New API/ISO Procedures for Proppant Testing. Paper SPE 110697 presented at the SPE Annual Technical Conference and Exhibition, Anaheim, California, USA, 11-17 November doi:10.2118/110697-MS.

Kim, C.M. and Losacano, J.A. 1985. Fracture Conductivity Damage Due to Crosslinked Gel Residue and Closure Stress on Propped 20/40 Mesh sand. Paper SPE 14436 presented at the SPE Annual Technical Conference and Exhibition, Las Vegas, Nevada, USA, 22-25 September doi:10.2118/14436-MS.

Marpaung, F. 2007. Investigation of the Effect of Gel Residue on Hydraulic Fracture Conductivity Using Dynamic Fracture Conductivity Test. MS thesis, Texas A&M University, College Station, Texas.

Marpaung, F., Chen, F., Pongthunya, P., Zhu, D., and Hill, A.D. 2008. Measurement of Gel Cleanup in a Propped Fracture with Dynamic Fracture Conductivity Experiments. Paper SPE 115653 presented at the SPE Annual Technical Conference and Exhibition, Denver, Colorado, USA, 21-24 September doi:10.2118/115653-MS.

McDaniel, B.W. 1986. Conductivity Testing of Proppants at High Temperature and Stress. Paper SPE 15067 presented at the SPE California Regional Meeting, Oakland, California, USA, 2-4 April doi:10.2118/15067-MS.

Milton-Tayler, D. 1993. Realistic Fracture Conductivities of Propped Hydraulic Fractures. Paper SPE 26602 presented at the SPE Annual Technical Conference and Exhibition, Houston, Texas, USA, 3-6 October doi:10.2118/26602-MS.

Montgomery, D.C. and Runger, G.C. 2003. *Applied Statistics and Probability for Engineers*. Hoboken, New Jersey: John Wiley & Sons, Inc.

Myers, R. and Montgomery, D. 2002. *Response Surface Methodology- Process and Product Optimization Using Designed Experiments*. Hoboken, New Jersey: John Wiley & Sons, Inc.

Palisch, T.T., Duenckel, R.J., Bazan, L.W., Heidt, J.H., and Turk, G.A. 2007. Determining Realistic Fracture Conductivity and Understanding Its Impact on Well Performance - Theory and Field Examples. Paper SPE 106301 presented at the SPE Hydraulic Fracturing Technology Conference, College Station, Texas, USA, 29-31 January doi:10.2118/106301-MS.

Pongthunya, P. 2007. Development, Setup and Testing of a Dynamic Hydraulic Fracture Conductivity Apparatus. MS thesis, Texas A&M University, College Station, Texas.

Schubarth, S. and Milton-Tayler, D. 2004. Investigating How Proppant Packs Change under Stress. Paper SPE 90562 presented at the SPE Annual Technical Conference and Exhibition, Houston, Texas, USA, 26-29 September doi:10.2118/90562-MS.

Terracina, J.M., Turner, J.M., Collins, D.H., and Spillars, S. 2010. Proppant Selection and Its Effect on the Results of Fracturing Treatments Performed in Shale Formations. Paper SPE 135502 presented at the SPE Annual Technical Conference and Exhibition, Florence, Italy, 19-22 September 10.2118/135502-MS.

van der Vlis, A.C., Haafkens, R., Schipper, B.A., and Visser, W. 1975. Criteria for Proppant Placement and Fracture Conductivity. Paper SPE 5637 presented at the Fall Meeting of the Society of Petroleum Engineers of AIME, Dallas, Texas, USA, 28 September-1 October doi:10.2118/5637-MS.

Volk, L.J., Gall, B.L., Raible, C.J., and Carroll, H.B. 1983. A Method for Evaluation of Formation Damage Due to Fracturing Fluids. Paper SPE 11638 presented at the SPE/DOE Low Permeability Gas Reservoirs Symposium, Denver, Colorado, USA, 14-16 March doi:10.2118/11638-MS.

Zahid, S., Bhatti, A.A., Khan, H.A., and Ahmad, T. 2007. Development of Unconventional Gas Resources: Stimulation Perspective. Paper SPE 107053 presented at the Production and Operations Symposium, Oklahoma City, Oklahoma, USA, 31 March-3 April doi:10.2118/107053-MS.

APPENDIX

A.1 Hydraulic Fracture Experiment Data Sheet

Data used for calculations

Length of fracture over pressure drop	5.25
Width of fracture face (in) =	1.75
RMM of nitrogen (kg / mole) =	0.028
Compressibility factor, Z =	1.00
R (J / mol K) =	8.3144
Temperature, T (K) =	293.15
Viscosity of nitrogen (Pa .s) =	1.75923E-05
Density of nitrogen (kg/m^3) =	1.16085
Standard pressure (psi) =	14.7
Overburden ram area (in^2) =	125
Rock surface area (in^2) =	12.00

Calibration Data

Pcell =	0	psi
ΔP Front =	0	psi
Load from Frame (psi) =	2000.00	psi
Proppant wieght		grm
Fracture Surface Area	12.00	sq in
Proppant Conc in the fracture	0.000	lb/sq ft
Polymer Loading		lbm/Mgal
Gas Rate		slm
Average Fracture width =		in

Calculations

Time (hrs)	Overburdern Pressure	Flow Rate	P_{Cell}	ΔP	y-axis, $(P_1^2-P_2^2)Mh/(2ZRTL\rho\mu_g)$	x-axis, $rq/h\mu$,	Intercept from Graph	k_f-w	Permeability
(hrs)	(psi)	(slm)	(psi)	(psi)	(1/m^3)	no unit		(md-ft)	(Darcy)
0	2000						#DIV/0!	#DIV/0!	#DIV/0!
2	2000						#DIV/0!	#DIV/0!	#DIV/0!
4	2000						#DIV/0!	#DIV/0!	#DIV/0!
6	2000						#DIV/0!	#DIV/0!	#DIV/0!
8	2000						#DIV/0!	#DIV/0!	#DIV/0!
10	2000						#DIV/0!	#DIV/0!	#DIV/0!
12	2000						#DIV/0!	#DIV/0!	#DIV/0!
15	2000						#DIV/0!	#DIV/0!	#DIV/0!
18	2000						#DIV/0!	#DIV/0!	#DIV/0!

Fig. A.1 Fracture conductivity experimental data spreadsheet

A.2 Calibration Setup Experimental Results

Table A.1 Experiment properties

Proppant loading	2	ppg
Polymer loading	10	lb/Mgal
Temperature	150	F
Use of Breaker	Yes	
Closure Stress	2000	psi
Gas flow rate	1	L/min
Proppant Concentration	0.25212	lbm/sq ft

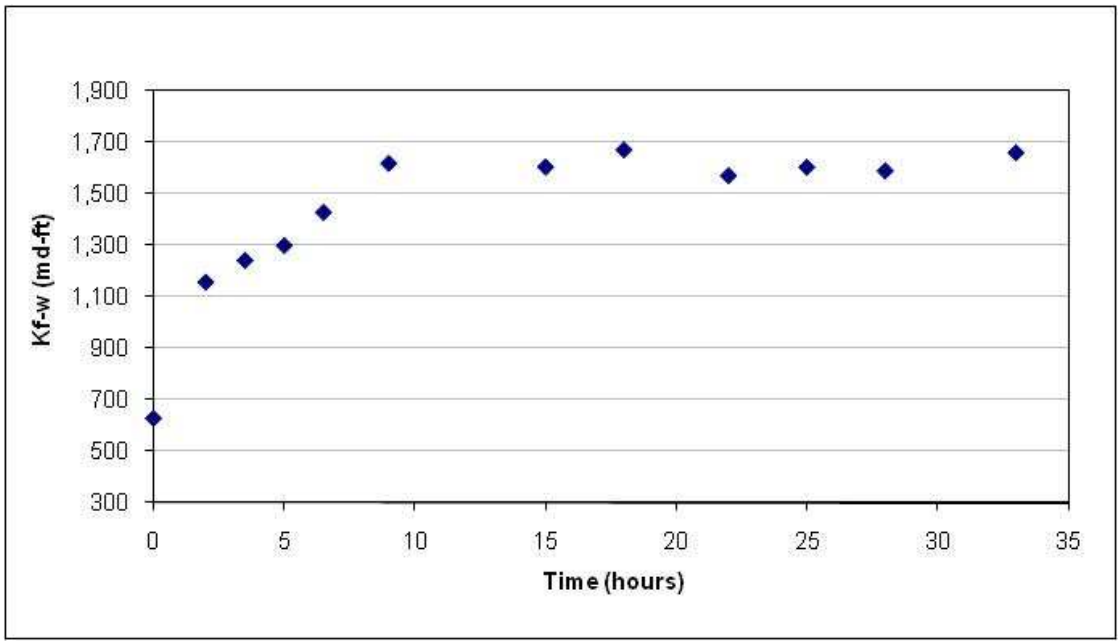

Fig. A.2 Calibration setup experimental results

A.3 Sieve Analysis Results

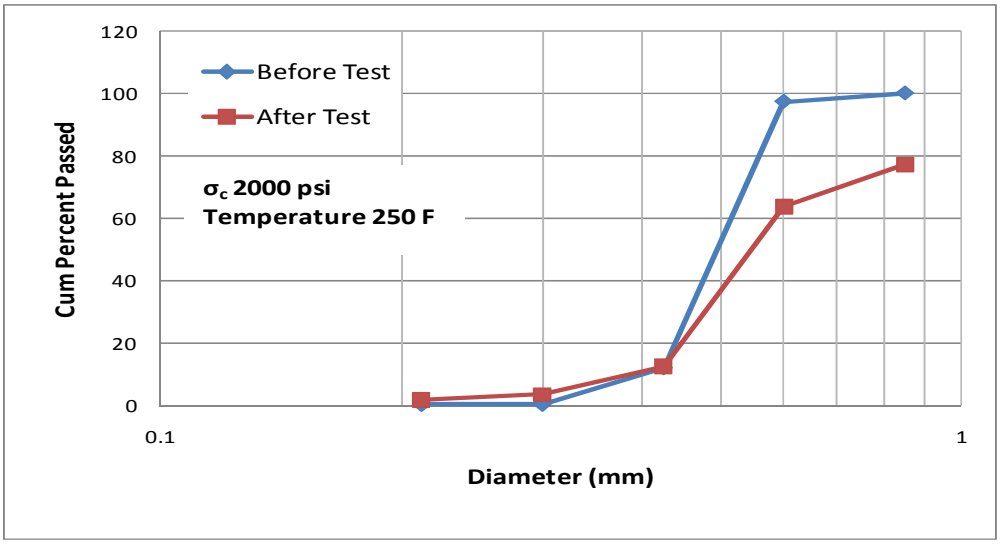

Fig. A.3 Sieve analysis results for 2000 psi and 250 F

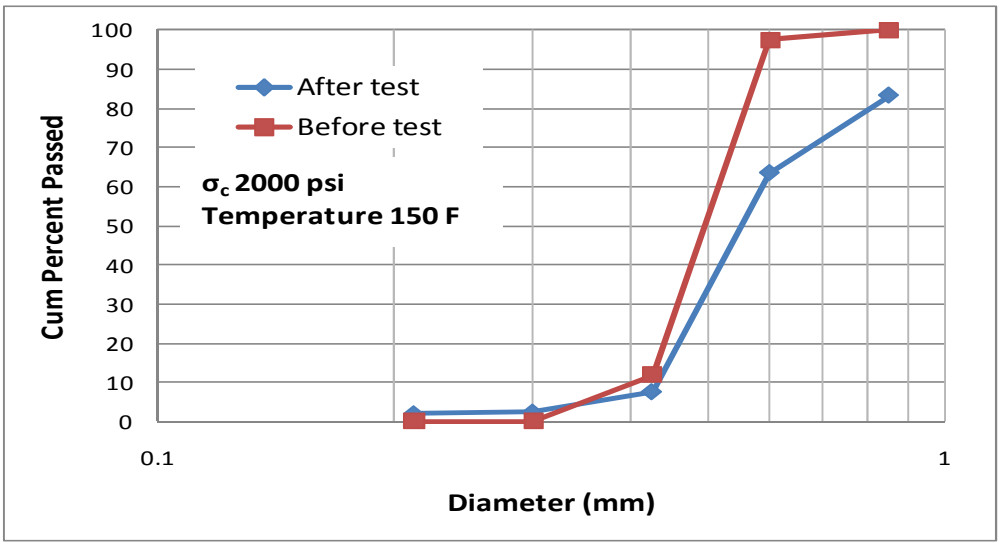

Fig. A.4 Sieve analysis results for 2000 psi and 150 F

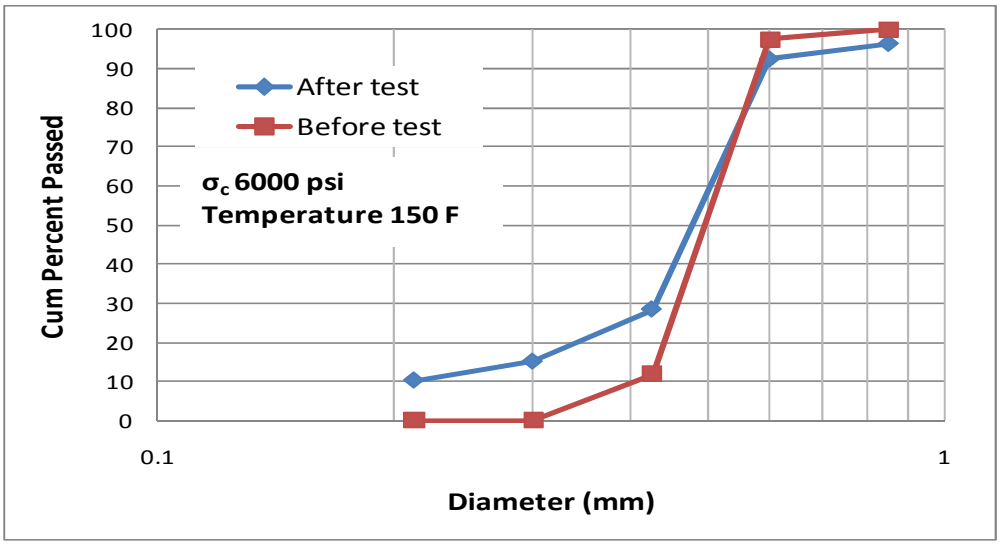

Fig. A.5 Sieve analysis results for 6000 psi and 150 F

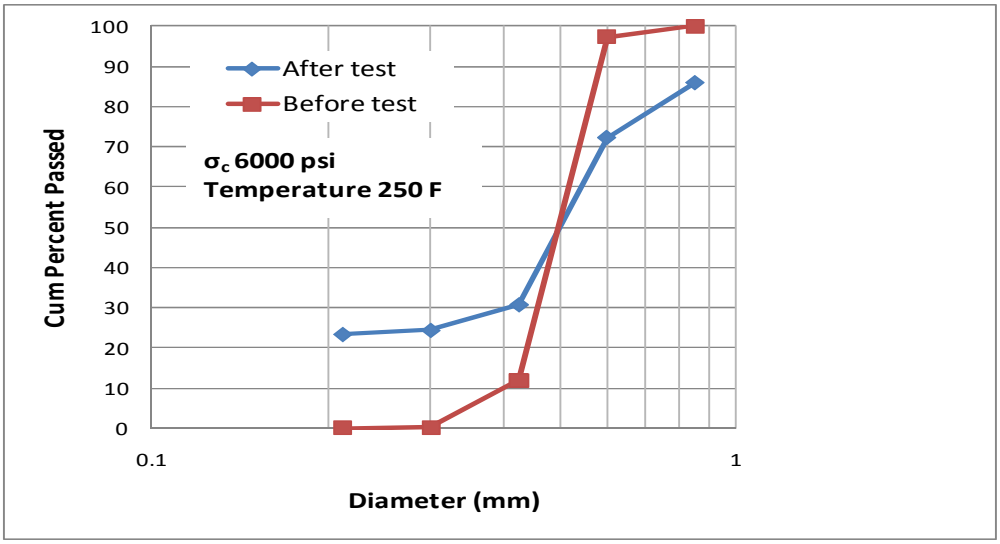

Fig. A.6 Sieve analysis results for 6000 psi and 250 F

VITA

Name: Andres Eduardo Pieve La Rosa

Address: 3116 TAMU 407
Department of Petroleum Engineering
College Station, Texas, 77843-3116
Phone: 979-229-0045

Email: pievex@gmail.com

Education: B.S., Petroleum Engineering
Universidad Central de Venezuela, 2007
Caracas, Venezuela

M.S., Petroleum Engineering
Texas A&M University, 2011
College Station, Texas, USA

This thesis was typed by the author.